An Uncertainty Partition Approach for Inferring Interactive Hydrologic Risks

Yurui Fan[1], Kai Huang[2], Guohe Huang[3], Yongping Li[4], Feng Wang[4]

[1] Department of Civil and Environmental Engineering, Brunel University, London, Uxbridge, Middlesex, UB8 3PH, United Kingdom
[2] Faculty of Engineering and Applied Sciences, University of Regina, Regina, SK, Canada, S4S0A2
[3] Institute for Energy, Environment and Sustainable Communities, University of Regina, Regina, Saskatchewan, Canada S4S 0A2
[4] School of Environment, Beijing Normal University, Beijing 100875, China

Correspondence to: Yurui Fan (yurui.fan@brunel.ac.uk), Guohe Huang (huangg@uregina.ca)

Abstract:

Extensive uncertainties exist in hydrologic risk analysis. Particularly for interdependent hydrometeorological extremes, the random features in individual variables and their dependence structures may lead to bias and uncertainty in future risk inferences. In this study, a full-subsampling factorial copula (FSFC) approach is proposed to quantify parameter uncertainties and further reveal their contributions to predictive uncertainties in risk inferences. Specifically, a full-subsampling factorial analysis (FSFA) approach is developed to diminish the effect of the sample size and provide reliable characterization for parameters' contributions to the resulting risk inferences. The proposed approach is applied to multivariate flood risk inference for Wei River basin to demonstrate the applicability of FSFC for tracking the major contributors to resulting uncertainty in a multivariate risk analysis framework. In detail, the multivariate risk model associated with flood peak and volume will be established and further introduced into the proposed full-subsampling factorial analysis framework to reveal the individual and interactive effects of parameter uncertainties on the predictive uncertainties in the resulting risk inferences. The results suggest that uncertainties in risk inferences would mainly be attributed to some parameters of the marginal distributions while the parameter of dependence structure

30   (i.e. copula function) would not produce noticeable effects. Moreover, compared with traditional

factorial analysis (FA), the proposed FSFA approach would produce more reliable visualization for

parameters' impacts on risk inferences, while the traditional FA would remarkable overestimate

contribution of parameters' interaction to the failure probability in AND, and at the same time,

underestimate the contribution of parameters' interaction to the failure probabilities in OR and Kendall.

35

1. Introduction

Many hydrological and climatological extremes are highly correlated among each other, and it is desired

to explore their interdependence through multivariate approaches. Examples include sea level rise and

40   fluvial flood (Moftakhari et al., 2017), drought and heat waves (Sun et al., 2019), soil moisture and

precipitation (AghaKouchak, 2015). Moreover, even one specific hydrological extreme may have

multiple attributes, such as the peak and volume for a flood, duration and severity for a drought, and

duration and intensity of a storm (Karmakar and Simonovic, 2009; Kong et al., 2019). Traditional

univariate approaches, mainly focusing on one variable or one attribute of hydrological extremes (e.g.

45   flood peak), may not be sufficient to describe those hydrological extemes containing multivariate

characteristics. Thus the univariate frequency/risk analysis methods may be unable to obtain reliable

risk inferences for the failure probability or recurrence intervals of interdependent extreme events

(Chebana and Ouarda, 2011; Requena et al., 2013; Salvadori et al., 2016; Sadegh et al., 2017)

50   Since the introduction of copula function into hydrology and geosciences by De Michele and Salvador

(2003), the copula-based approaches have been widely used for multivariate hydrologic risk analysis.

The copula functions are able to model correlated variables with complex or nonlinear dependence

structures. Also, this kind of methods are easily to be implemented since the marginal distributions and

dependence model can be estimated in separate processes, which also give flexibility in selection of

55   both marginal and dependence models. A great number of research has been developed for multivariate

hydrologic simulation through copula functions, such as multivariate flood frequency analysis (Sraj et

al., 2014; Xu et al., 2016; Fan et al., 2018); drought assessments (Song and Singh 2010; Kao and

Govindaraju 2010; Ma et al. 2013); storm or rainfall dependence analysis (Zhang and Singh 2007;

Vandenberghe et al. 2010); streamflow simulation (Lee and Salas 2011; Kong et al., 2015) and other

60   water and environmental engineering applications (Fan et al., 2017; Huang et al., 2017).

For both univariate and multivariate analysis for hydrometeorological risks, uncertainty would be one of

the unavoidable issues which needs to be well addressed. The uncertainty in hydrometeorological risk

inference mainly results from stochastic variability of hydrometeorological processes and incomplete

65   knowledge of the watershed systems (Merz and Thieken, 2005). Amounts of studies have been proposed

to address uncertainty in both univariate and multivariate hydrological risk analysis (e.g. Merz and

Thieken, 2005; Serinaldi, 2013; Dung et al., 2015; Zhang et al., 2015; Sadegh et al., 2017; Fan et al.,

2018). However, one critical issue in uncertainty quantification of hydrological inference is how to

characterize the major sources for uncertain risk inference. Qi et al. (2016) employed a subsampling

70   ANOVA approach (Bosshard et al., 2013), to quantify individual and interactive impacts of the

uncertainties in data, probability distribution functions and probability distribution parameters on the

total cost for flood control in terms of flood peak flows. Even though the subsampling ANOVA

approach is able to reduce the effect of the biased estimator on quantification of variance contribution

resulting from traditional ANOVA approach, it would be noticed that merely subsampling one

75   uncertainty parameter/factor (referred as single-subsampling ANOVA), as used in the studies by

Bosshard et al. (2013) and Qi et al. (2016a), will lead to underestimation of individual contribution for

the factor to be sampled and overestimation of contributions for those non-sampled factors. Moreover,

few studies have been reported to characterize the individual and interactive effects of parameter

uncertainties in marginal and dependence models on the multivariate risk inferences.

Consequently, as an extension of previous research, this study aims to propose a Full-subsampling factorial copula (FSFC) approach for uncertainty quantification and partition in multivariate hydrologic risk inference. In detail, the parameter uncertainties are quantified through a Monte Carlo-based Bootstrap algorithm. The interactions of parameter uncertainties are explored through a multilevel factorial analysis approach. The contributions of parameter uncertainties are analyzed through a full-subsampling factorial analysis (FSFA) method, in which all uncertain factors will be subsampled to generate more reliable results. The applicability of the proposed FSFC approach will demonstrated through case studies of flood risk analysis in the Wei River basin in China.

2. Methodology

Figure 1 illustrates the framework of the proposed FSFC approach. The framework consists of four modules: (i) selection of marginal distributions, (ii) identification of copulas, (iii) parameter uncertainty quantification, (iv) parameter interaction and sensitivity analysis. In FSFC, modules (i) and (ii) are proposed to construct the most appropriate copula-based hydrologic risk model. Module (iii) quantifies parameter uncertainties in marginal distributions and copulas. Modules (iv) would be the core part of our study to identify the main sources of uncertainties in multivariate risk inference by the proposed full-subsampling factorial analysis (FSFA) approach.

Place Figure 1 here

2.2. Copula-based Multivariate Risk Inference Framework

105   A copula function is a multivariate distribution function with uniform margins on the interval [0, 1].

Sklar's Theorem states that any d-dimensional distribution function F can be formulated through a

copula and its marginal distributions (Nelsen, 2006). In detail, a multivariate copula function can be

expressed as:

$$F(x_1, x_2, ..., x_d \mid \gamma_1, \gamma_2, ..., \gamma_d, \theta) = C(F_{X_1}(x_1 \mid \gamma_1), F_{X_2}(x_2 \mid \gamma_2), ..., F_{X_d}(x_d \mid \gamma_d) \mid \theta) \qquad (1)$$

110   where $F_{X_1}(x_1 \mid \gamma_1), F_{X_2}(x_2 \mid \gamma_2), ..., F_{X_d}(x_d \mid \gamma_d)$ are marginal distributions of the random vector $(X_1, X_2, …,$

$X_d)$, with $\gamma_1, \gamma_2, …, \gamma_d$ respectively being the unknow parameters of marginal distributions. θ is the

parameter in the copula function describing dependence among the correlated variables. If these

marginal distributions are continuous, then a single copula function C exists, which can be written as

(Nelsen, 2006):

115    $$C(u_1, u_2, ..., u_d \mid \theta) = F(F_{X_1}^{-1}(u_1 \mid \gamma_1), F_{X_2}^{-1}(u_2 \mid \gamma_2), ..., F_{X_d}^{-1}(u_d \mid \gamma_d)) \qquad (2)$$

where $u_1 = F_{X_1}(x_1 \mid \gamma_1)$, $u_2 = F_{X_2}(x_2 \mid \gamma_2)$, …, $u_d = F_{X_d}(x_d \mid \gamma_d)$. More details on the theoretical

background and properties of various copula families can be found in Nelsen (2006).

If appropriate copula functions are specified to reflect the joint probabilistic characteristics ~~among~~ for a

120   multivariate extreme event, the conditional, primary and secondary return periods (RP) can be obtained.

Consider one kind of hydrological extreme (denoted as X) with d attributes (i.e. $X = (x_1, x_2, …, x_d)$), and

for a specific extreme event X^* with its attributes being $X^* = (x_1^*, x_2^*, …, x_d^*)$, three categories of

multivariate RP can be applied to determine ~~for revealing~~ the potential risk of X^*.

There is something missing here. Please introduce your 'OR' and 'AND' cases to assist the reader. Also, what are the names of T^{OR} and T^{AND}? what do they describe? What is R^d?

125   (i) "OR" case:

Hydrology and
Earth System
Sciences
Discussions

Open Access

EGU

$$T^{OR} = \{(x_1, x_2, ..., x_d) \in R^d : x_1 > x_1^* \vee x_2 > x_2^* \vee ... \vee x_d > x_d^*\}$$

$$= \frac{\mu}{1 - C(F_1(x_1 \mid \gamma_1), ..., F_d(x_d \mid \gamma_d) \mid \theta)} \tag{4}$$

where μ denotes the average time between two adjacent events under consideration.

(ii) "AND" case:

$$T^{AND} = \{(x_1, x_2, ..., x_d) \in R^d : x_1 > x_1^* \wedge x_2 > x_2^* \wedge ... \wedge x_d > x_d^*\}$$

130

$$= \frac{\mu}{\hat{C}(\overline{F}_1(x_1 \mid \gamma_1), \overline{F}_2(x_2 \mid \gamma_2), ..., \overline{F}_1(x_d \mid \gamma_d) \mid \theta)} \tag{5}$$

where $\hat{C}$ is the multivariate survival function of the X_i's proposed by Salvadori et al. (2013; 2016),

and $\overline{F}_i(x_i \mid \gamma_i) = P(X > x_i) = 1 - F_i(x_i \mid \gamma_i)$. Following Salvadori et al. (2013; 2016), and the Inclusion-

Exclusion principle proposed by Joe (2014), the multivariate survival function $\hat{C}$ can be obtained by:

$$\hat{C}(\mathbf{u}) = \overline{C}(1 - \mathbf{u}) \tag{6}$$

135   and

what is this?

$$\overline{C}(\mathbf{u}) = 1 - \sum_{i=1}^{d} u_i + \sum_{S \in P} (-1)^{\#(S)} C_S(u_i : i \in S) \tag{7}$$

(iii) "Kendall" case: The Kendall RP characterizes the hydrologic disasters exceeding a critical layer as

defined by (Salvadori et al., 2011): $L_t^F = \{\mathbf{x} \in R^d : F(\mathbf{x}) = t\}$. The Kendall RP can be expressed as

140   (Salvadori et al., 2011):

$$T^{Kendall} = \frac{\mu}{1 - K_C(t)} \tag{8}$$

where K_C is the Kendall distribution function associated with C, which can be expressed as:

$$K_C(t) = P(C(F_1(x_1 \mid \gamma_1), ..., F_d(x_d \mid \gamma_d) \mid \theta) \leq t) \tag{9}$$

145   In addition to the multivariate RP, Failure probability (FP) can be another index to provide more

coherent, general and well devised tools for multivariate risk assessment and communication. In

general, the failure probability p_M to indicate the occurrence of a critical event for at least one time in M

years of design life can be defined as (Salvadori et al., 2016):

$$p_M = 1 - \prod_{j=1}^{M}(1 - p_j) = 1 - (F(x_d))^M \tag{10}$$

150   Similar to the multivariate RP concept, the failure probability in a multivariate context can also be

characterized in "OR", "AND", and "Kendall" scenarios expressed by the following equations. For a

given critical threshold $x^* = \{x_1^*, x_2^*, ..., x_d^*\}$, the failure probabilities violating this critical value can be

expressed as (Salvadori et al., 2016):

$$p_T^{OR} = 1 - (C(F_1(x_1^* \mid \gamma_1), F_1(x_2^* \mid \gamma_2), ..., F_d(x_d^* \mid \gamma_d) \mid \theta))^T \tag{11a}$$

155    $$p_T^{AND} = 1 - (1 - \hat{C}(\overline{F}_1(x_1^* \mid \gamma_1), \overline{F}_2(x_2^* \mid \gamma_2), ..., \overline{F}_1(x_d^* \mid \gamma_d) \mid \theta))^T \tag{11b}$$

$$p_T^{Kendall} = 1 - (P(C(F_1(x_1^* \mid \gamma_1), F_1(x_2^* \mid \gamma_2), ..., F_d(x_d^* \mid \gamma_d) \mid \theta) \leq t))^T \tag{11c}$$

where p_T^{OR}, p_T^{AND}, and $p_T^{Kendall}$ respectively denote the failure probability in "AND", "OR" and

"Kendall" cases. T indicates the service time of the facilities under consideration.

160   Focusing on a bivariate case, the joint RP and the associate failure probability in "OR", "AND", and

"Kendall" scenarios can be formulated as (Salvadori et al., 2007, 2011; Graler et al., 2013; Sraj et al.,

2014; Serinaldi, 2015):

$$T_{u_1,u_2}^{OR} = \frac{\mu}{1 - C_{U_1U_2}(u_1, u_2 \mid \theta)} \tag{12a}$$

$$T_{u_1,u_2}^{AND} = \frac{\mu}{1-u_1-u_2+C_{U_1U_2}(u_1,u_2 \mid \theta)} \tag{12b}$$

165

$$T_{u_1,u_2}^{Kendall} = \frac{\mu}{1-P(C_{U_1U_2}(u_1^*,u_2^*) \le t)} \tag{12c}$$

$$p_T^{OR} = 1-(C_{U_1U_2}(u_1^*,u_2^* \mid \theta))^T \tag{12d}$$

$$p_T^{AND} = 1-(u_1^* + u_2^* - \hat{C}_{U_1U_2}(u_1^*,u_2^* \mid \theta))^T \tag{12e}$$

$$p_T^{Kendall} = 1-(P(C_{U_1U_2}(u_1^*,u_2^* \mid \theta) \le t))^T \tag{12f}$$

where $u_1 = F_1(x_1 \mid \gamma_1), u_2 = F_2(x_2 \mid \gamma_2)$, $u_1^* = F_1(x_1^* \mid \gamma_1), u_2^* = F_2(x_2^* \mid \gamma_2)$, (x_1^*, x_2^*) defines the bivariate

170   threshold.

2.3. Uncertainty in the Copula-base Risk Model

175   Extensive uncertainties may be involved in the parametric estimation of a copula function due to: (i) the

inherent uncertainty in the flooding process; (ii) uncertainty in the selection of appropriate marginal

functions and copulas; and, (iii) statistical uncertainty or parameter uncertainty within the parameter

estimation process (e.g. the availability of samples) (Zhang et al., 2015). Several methods have been

proposed to quantify parameter uncertainties in copula-based models. For instance, Dung et al. (2015)

180   proposed bootstrap-based methods for quantifying the parameter uncertainties in bivariate copula

models. Zhang et al. (2015) employed a Bayesian inference approach for evaluating uncertainties in

copula-based hydrologic droughts models, in which the Component-wise Hit-And-Run Metropolis

algorithm is adopted to estimate the posterior probabilities of model parameters.

185 In this study, a bootstrap-based algorithm, will be applied to quantify parameter uncertainties in the copula-based multivariate risk model. The procedures the bootstrap-based algorithm to derive probabilistic distributions of the parameters in both marginal and dependence models are presented as follows:

1. Predefine a large number of bootstrapping samplings N_B

190 2. Implement the resampling with replacement over observed pairs $Z = (X, Y)$ to obtain $Z^* = (X^*, Y^*)$; Z^* has the same size as Z.

3. Fit the chosen marginal distributions to X^* and Y^*, and estimate the associated parameters (γ_X, γ_Y).

4. Fit the chosen copula to Z^*, and estimate the parameter in the copula function θ.

5. Repeat step 2–5 N_B times, and obtain N_B sets of $(\gamma_X, \gamma_Y, \theta)$. Moreover, the reject those parameters

195 that lead to bad fits for both marginal and copula models, the A-D test and the Cramer-von-Mises test are introduced in the bootstrap procedure to ensure that the obtained parameters can pass statistic tests for both the marginal distribution and copula models. Then the kernel method will be adopted to quantify the probabilistic features for $\gamma_X, \gamma_Y, \theta$.

6. In order to derive bivariate uncertainty bands for a predefined quantile curve (QC) with certain joint

200 RP in 'AND', 'OR' or 'Kendall' (denoted as T^{AND}, T^{OR}, $T^{Kendall}$), sample N_{B_1} sets of $(\gamma_X, \gamma_Y, \theta)$ from the obtained N_B samples

7. Sample a large number (N_s) of x_i y_j from their marginal distributions.

8. For each set of $(\gamma_X, \gamma_Y, \theta)$ from N_{B_1}, evaluate the joint RPs of (x_i, y_j) ($i = 1, 2, …, N_s$; $y = 1, 2, …,$ N_s), and store the pairs of (x_i, y_j) approaching the predefined joint RPs.

205 9. Repeat step 8 for N_{B_1}, and for each predefined QC, and plot the bivariate uncertainty bands for each quantile QC

Hydrology and
Earth System
Sciences
Discussions

Open Access

EGU

2.4. Interactive and Sensitivity Analysis for Parameter Uncertainties

210   Due to the uncertainties existing in the unknown parameters for a copula model, the associated risk or

the return period for a flooding event may also be uncertain. Few studies have been reported to analyze

the effect of uncertainties in the copula model on evaluating the risk for a flood event. To address the

above issue, a full-subsampling factorial analysis (FSFA) approach will be proposed to reveal the

individual and interactive effects of parameter uncertainties on the predictive uncertainties of different

215   risk inferences.

Consider a copula-based bivariate risk assessment model which has two marginal distributions (*A* and

B) and one copula (*C*). The parameters in the two marginal distributions are assumed to be respectively

denoted as γ^A with *a* levels and γ^B with b levels, while the parameter in the copula is denoted with θ^C

220   with *c* levels. The three factor ANOVA model for such a factorial design in terms of the predictive risk

(denoted as *R*) in response to the parameters γ_A, γ_B, θ_C and *n* replicates, can be expressed as:

$$R_{ijkl} = R_0 + R_{\theta_i^C} + R_{\gamma_j^A} + R_{\gamma_k^B} + R_{\theta_i^C \gamma_j^A} + R_{\theta_i^C \gamma_k^B} + R_{\gamma_j^A \gamma_k^B} + R_{\theta_i^C \gamma_j^A \gamma_k^B} + \varepsilon_{ijkl} \begin{cases} i = 1, 2, ..., c \\ j = 1, 2, ..., a \\ k = 1, 2, ...b \\ l = 1, 2, ..., n \end{cases} \quad (13)$$

where R_0 denotes the overall mean effect; $R_{\theta_i^C}, R_{\gamma_j^A}, R_{\gamma_k^B}$ respectively indicate the effect for parameter θ^C

225   in the copula at the *i*th level, parameter γ^A in the first marginal distribution at the *j*th level, and parameter

γ^B in the first marginal distribution at the *k*th level; $R_{\theta_i^C \gamma_j^A}, R_{\theta_i^C \gamma_k^B}, R_{\gamma_j^A \gamma_k^B}$ indicate interactions between

factors θ^C and γ^A, θ^C and γ^B, as well as γ^A and γ^B, respectively; $R_{\theta_i^C \gamma_j^A \gamma_k^B}$ denotes the interaction of factors

θ^C , γ^A and γ^B; ε_{ijkl} denotes the random error component.

230   Based on Equation (13), the total variability of the predictive risk can be decomposed into its

component parts as follows (Montgomery, 2001):

$$SS_T = SS_{\theta^C} + SS_{\gamma^A} + SS_{\gamma^B} + SS_I + SS_e \qquad (14a)$$

and

235    $$SS_T = \sum_{i=1}^{c}\sum_{j=1}^{a}\sum_{k=1}^{b}\sum_{l=1}^{n} R_{ijkl}^2 - \frac{R_{....}^2}{abcn} \qquad (14b)$$

$$SS_{\theta^C} = \frac{1}{abn}\sum_{i=1}^{c} R_{i...}^2 - \frac{R_{....}^2}{abcn} \qquad (14c)$$

$$SS_{\gamma^A} = \frac{1}{bcn}\sum_{j=1}^{a} R_{.j..}^2 - \frac{R_{....}^2}{abcn} \qquad (14d)$$

$$SS_{\gamma^B} = \frac{1}{acn}\sum_{k=1}^{b} R_{..k.}^2 - \frac{R_{....}^2}{abcn} \qquad (14e)$$

$$SS_e = \sum_{i=1}^{c}\sum_{j=1}^{a}\sum_{k=1}^{b}\sum_{l=1}^{n} R_{ijkl}^2 - \frac{1}{n}\sum_{i=1}^{c}\sum_{j=1}^{a}\sum_{k=1}^{b} R_{ijk.}^2 \qquad (14f)$$

$$SS_I = SS_{\theta^C\gamma^A} + SS_{\theta^C\gamma^B} + SS_{\gamma^B\gamma^A} + SS_{\theta^C\gamma^A\gamma^B}$$
240
$$= SS_T - SS_{\theta^C} - SS_{\gamma^A} - SS_{\gamma^B} - SS_e \qquad (14g)$$

where $R_{ijk.} = \sum_{l=1}^{n} R_{ijkl}$, $R_{i...} = \sum_{j=1}^{a}\sum_{k=1}^{b}\sum_{l=1}^{n} R_{ijkl}$, $R_{.j..} = \sum_{i=1}^{c}\sum_{k=1}^{b}\sum_{l=1}^{n} R_{ijkl}$, $R_{..k.} = \sum_{i=1}^{c}\sum_{j=1}^{a}\sum_{l=1}^{n} R_{ijkl}$

$R_{....} = \sum_{i=1}^{c}\sum_{j=1}^{a}\sum_{k=1}^{b}\sum_{l=1}^{n} R_{ijkl}$. Then the contributions of parameter uncertainties in marginal

distributions and dependence structures can be calculated as:

245   (1) Contribution of parameters in marginal distributions A and B

$$\eta_A = SS_{\gamma^A} / SS_T \tag{15a}$$

$$\eta_B = SS_{\gamma^B} / SS_T \tag{15b}$$

(2) Contribution of the parameter in the dependence structure

$$\eta_C = SS_{\theta^C} / SS_T \tag{15c}$$

250   (3) Contribution of internal variability

$$\eta_e = SS_e / SS_T \tag{15d}$$

(4) Contribution of parameter interactions

$$\eta_I = 1 - \eta_A - \eta_B - \eta_C - \eta_e \tag{15e}$$

255   However, one major issue for ANOVA approach is that the biased variance estimator in ANOVA would underestimate the variance in small sample size scenarios (Bosshard et al., 2013). Thus the sample size may significantly affect the resulting variance contributions expressed in Equations (15a) – (15e). A subsampling approach has been advanced by Bosshard et al. (2013) to diminish the effect of the sample size in ANOVA and has been employed for uncertainty partition in flood design and hydrological

260   simulation (Qi et al., 2016a, b). In such a subsampling scheme, one factor (denoted as X) with T levels (these levels can be different values for numerical parameters, or different types for non-numerical factor (e.g. model type)), would choose two levels in each iteration. For T possible levels of X, we can obtain a total of C_T^2 possible pairs for X, expressed as a $2 \times C_T^2$ matrix as follows:

265
$$g(h, j) = \begin{pmatrix} X_1 & X_1 & \cdots & X_1 & X_2 & X_2 & \cdots & X_{T-2} & X_{T-2} & X_{T-1} \\ X_2 & X_3 & \cdots & X_T & X_3 & X_4 & \cdots & X_{T-1} & X_T & X_T \end{pmatrix} \tag{16}$$

However, such a subsampling approach mainly applied to subsample merely one factor or one

parameter (here we refer to this method as single-subsampling ANOVA) in previous studies (Bosshard et al. 2013; Qi et al., 2016a, b). However, one critical issue for the single-subsampling ANOVA it that it

270   will lead to underestimation of individual contribution for the factor to be sampled and overestimation of contributions for those non-sampled factors. Consequently, in this study, we will propose a FSFA approach to subsample all the factors to be addressed, and then quantify the contribution of each factor to the response variation. In the FSFA approach, all factors under consideration will be subsampled, and the corresponding sum of squares will be obtained. The contribution of one factor would be

275   characterized by the mean value of its contribution in each iteration. In detail, for the three factor ANOVA model expressed by Equation (13), the subsampling schemes for the three parameters can be formulated as:

$$g_{\theta^C}(h_C, j_C) = \begin{pmatrix} \theta_1^C & \theta_1^C & \cdots & \theta_1^C & \theta_2^C & \theta_2^C & \cdots & \theta_{c-2}^C & \theta_{c-2}^C & \theta_{c-1}^C \\ \theta_2^C & \theta_3^C & \cdots & \theta_c^C & \theta_3^C & \theta_4^C & \cdots & \theta_{c-1}^C & \theta_c^C & \theta_c^C \end{pmatrix} \tag{17a}$$

$$g_{\gamma^A}(h_A, j_A) = \begin{pmatrix} \gamma_1^A & \gamma_1^A & \cdots & \gamma_1^A & \gamma_2^A & \gamma_2^A & \cdots & \gamma_{a-2}^A & \gamma_{a-2}^A & \gamma_{a-1}^A \\ \gamma_2^A & \gamma_3^A & \cdots & \gamma_a^A & \gamma_3^A & \gamma_4^A & \cdots & \gamma_{a-1}^A & \gamma_a^A & \gamma_a^A \end{pmatrix} \tag{17b}$$

$$g_{\gamma^B}(h_B, j_B) = \begin{pmatrix} \gamma_1^B & \gamma_1^B & \cdots & \gamma_1^B & \gamma_2^B & \gamma_2^B & \cdots & \gamma_{b-2}^B & \gamma_{b-2}^B & \gamma_{b-1}^B \\ \gamma_2^B & \gamma_3^B & \cdots & \gamma_b^B & \gamma_3^B & \gamma_4^B & \cdots & \gamma_{b-1}^B & \gamma_b^B & \gamma_b^B \end{pmatrix} \tag{17c}$$

Consequently, there are a total number of $C_c^2 C_a^2 C_b^2$ iterations in FSFA for the three-factor model expressed as Equation (13). For each iteration, the sums of squares can be reformulated as:

285    $$SS_T^j = \sum_{h_C=1}^{2} \sum_{h_A=1}^{2} \sum_{h_B=1}^{2} \sum_{l=1}^{n} R_{g_{\theta^C}(h_C,j_C)g_{\gamma^A}(h_A,j_A)g_{\gamma^B}(h_B,j_B)l}^2 - \frac{R_{g_{\theta^C}(o,j_C)g_{\gamma^A}(o,j_A)g_{\gamma^B}(o,j_B).}^2}{8n} \tag{18a}$$

$$SS_{\theta^C}^j = \frac{1}{4n} \sum_{h_C=1}^{2} R_{g_{\theta^C}(h_C,j_C)g_{\gamma^A}(o,j_A)g_{\gamma^B}(o,j_B).}^2 - \frac{R_{g_{\theta^C}(o,j_C)g_{\gamma^A}(o,j_A)g_{\gamma^B}(o,j_B).}^2}{8n} \tag{18b}$$

Hydrology and
Earth System
Sciences
Discussions
Open Access
EGU

$$SS_{\gamma^A}^j = \frac{1}{4n} \sum_{h_A=1}^{2} R_{g_{\theta^C}(h_C,o)g_{\gamma^A}(h_A,j_A)g_{\gamma^B}(o,j_B).}^2 - \frac{R_{g_{\theta^C}(o,j_C)g_{\gamma^A}(o,j_A)g_{\gamma^B}(o,j_B).}^2}{8n} \tag{18c}$$

$$SS_{\gamma^B}^j = \frac{1}{4n} \sum_{h_B=1}^{2} R_{g_{\theta^C}(h_C,o)g_{\gamma^A}(o,j_A)g_{\gamma^B}(h_B,j_B).}^2 - \frac{R_{g_{\theta^C}(o,j_C)g_{\gamma^A}(o,j_A)g_{\gamma^B}(o,j_B).}^2}{8n} \tag{18d}$$

$$SS_e^j = \sum_{h_C=1}^{2}\sum_{h_A=1}^{2}\sum_{h_B=1}^{2}\sum_{l=1}^{n} R_{g_{\theta^C}(h_C,j_C)g_{\gamma^A}(h_A,j_A)g_{\gamma^B}(h_B,j_B)l}^2 - \frac{1}{n}\sum_{h_C=1}^{2}\sum_{h_A=1}^{2}\sum_{h_B=1}^{2} R_{g_{\theta^C}(h_C,j_C)g_{\gamma^A}(h_A,j_A)g_{\gamma^B}(h_B,j_B).}^2 \tag{18e}$$

290 $$SS_I^j = SS_T^j - SS_{\theta^C}^j - SS_{\gamma^A}^j - SS_{\gamma^B}^j - SS_e^j \tag{18f}$$

where

$$R_{g_{\theta^C}(h_C,j_C)g_{\gamma^A}(h_A,j_A)g_{\gamma^B}(h_B,j_B).} = \sum_{l=1}^{n} R_{g_{\theta^C}(h_C,j_C)g_{\gamma^A}(h_A,j_A)g_{\gamma^B}(h_B,j_B)l}$$

$$R_{g_{\theta^C}(h_C,j_C)g_{\gamma^A}(o,j_A)g_{\gamma^B}(o,j_B).} = \sum_{h_A=1}^{2}\sum_{h_B=1}^{2}\sum_{l=1}^{n} R_{g_{\theta^C}(h_C,j_C)g_{\gamma^A}(h_A,j_A)g_{\gamma^B}(h_B,j_B)l} \cdot$$

295 $$R_{g_{\theta^C}(o,j_C)g_{\gamma^A}(h_A,j_A)g_{\gamma^B}(o,j_B).} = \sum_{h_C=1}^{2}\sum_{h_B=1}^{2}\sum_{l=1}^{n} R_{g_{\theta^C}(h_C,j_C)g_{\gamma^A}(h_A,j_A)g_{\gamma^B}(h_B,j_B)l}$$

$$R_{g_{\theta^C}(o,j_C)g_{\gamma^A}(o,j_A)g_{\gamma^B}(h_B,j_B).} = \sum_{h_C=1}^{2}\sum_{h_A=1}^{2}\sum_{l=1}^{n} R_{g_{\theta^C}(h_C,j_C)g_{\gamma^A}(h_A,j_A)g_{\gamma^B}(h_B,j_B)l}$$

$$R_{g_{\theta^C}(o,j_C)g_{\gamma^A}(o,j_A)g_{\gamma^B}(o,j_B).} = \sum_{h_C=1}^{2}\sum_{h_A=1}^{2}\sum_{h_B=1}^{2}\sum_{l=1}^{n} R_{g_{\theta^C}(h_C,j_C)g_{\gamma^A}(h_A,j_A)g_{\gamma^B}(h_B,j_B)l}$$

Also, for each iteration, the corresponding contributions for each factor can be obtained as:

300 $$\eta_A^j = SS_{\gamma^A}^j \big/ SS_T^j \tag{19a}$$

$$\eta_B^j = SS_{\gamma^B}^j \big/ SS_T^j \tag{19b}$$

$$\eta_C^j = SS_{\theta^C}^j \big/ SS_T^j \tag{19c}$$

$$\eta_e^j = SS_e^j \big/ SS_T^j \tag{19d}$$

$$\eta_I^j = 1 - \eta_A^j - \eta_B^j - \eta_C^j - \eta_e^j \tag{19e}$$

Hydrology and
Earth System
Sciences
Discussions

Open Access

EGU

Finally, the individual and interactive contributions for those factors can be obtained by averaging the corresponding contributions in all iterations, expressed as:

$$\eta_A = \frac{1}{J}\sum_{j=1}^{J} SS_{\gamma^A}^{j} \Big/ SS_T^{j} \tag{20a}$$

$$\eta_B = \frac{1}{J}\sum_{j=1}^{J} SS_{\gamma^B}^{j} \Big/ SS_T^{j} \tag{20b}$$

$$\eta_C = \frac{1}{J}\sum_{j=1}^{J} SS_{\theta^C}^{j} \Big/ SS_T^{j} \tag{20c}$$

$$\eta_e = \frac{1}{J}\sum_{j=1}^{J} SS_{e}^{j} \Big/ SS_T^{j} \tag{20d}$$

$$\eta_I = \frac{1}{J}\sum_{j=1}^{J} \eta_I^{j} \tag{20e}$$

where $J = C_c^2 C_a^2 C_b^2$

3. Applications

The proposed FSFC approach can be applied for various multivariate risk inference problems. In this study, we will apply FSFC for multivariate flood risk inference at the Wei River basin in China. The Weihe River plays a key role in the economic development of western China, and thus is known regionally as the 'Mother River' of the Guanzhong Plain of the southern part of the loess plateau (Song et al. 2007; Zuo et al. 2014; Du et al. 2015, Xu et al., 2016). It originates from the Niaoshu Mountain at an elevation of 3485 m above mean sea level in Weiyuan County of Gansu Province (Du et al. 2015). The Weihe River basin is characterized by a semi-arid and sub-humid continental monsoon climate, resulting in significant temporal-spatial variations in precipitation, with an annual precipitation of 559 mm (Xu et al., 2016). Furthermore, there is a strong decreasing gradient from south to north, in which

the southern region experiences a sub-humid climate with annual precipitation ranging from 800 to

325   1000 mm, whereas the northern region has a semi-arid climate with annual precipitation ranging from

400 to 700 mm (Xu et al., 2016). Over the entire basin, the mean temperature ranges from 6 to 14 ^{0}C,

the annual potential evapotranspiration fluctuates from 660 to 1,600, and the annual actual

evapotranspiration is about 500 mm (Du et al. 2015).

330   Observed daily streamflow data at Xianyang and Zhangjiashan gauging stations are applied for

hydrologic risk analysis. Figure 1 show the locations of these three gauging stations. Based on the daily

stream flow data, the flood peak applied is defined as the maximum daily flow over a period and the

associated flood volume is considered as the cumulative flow during the flood period. In this study, the

flood characteristics are obtained based on an annual scale. This means that one flood event is identified

335   in each year. The detailed method to identify the flood peak and the associated flood volume can be

found in Yue (2000, 2001). Table 1 shows some descriptive statistical values for the considered

variables (peak discharge, Q; hydrograph volume, V), in which 47 and 55 flood events are characterized

at the Xianyang and Zhangjiashan station, respectively.

340   ---------------------------------
Place Figure 2 and Table 1 here
----

4. Results Analysis

345   ### 4.1. Model Evaluation and Selection

There are a number of potential probabilistic models for modelling individual flood variables and their

dependence structures. In this study, five alternative distributions, including gamma, generalized

extreme value (GEV), lognormal (LN), Pearson type III (P III), and log-Pearson type III (LP III)

350   distributions, are employed to describe the probabilistic features of the chosen flood variables (i.e. peak

and volume). Moreover, goodness-of-fit tests are performed through the indices of Kolmogorov-

Smirnov test (K-S test), root mean square error (RMSE) and Akaike Information Criterion (AIC), to

screen the performance of those potential models. The results are presented in Table 2. The results

indicate that all five parametric distributions can produce satisfactory results, with all p-values larger

355   than 0.05. However, it can be concluded that the GEV and lognormal approaches show best

performance for respectively modelling flood peak and volume at both gauging stations.

Place Tables 2 here

360   ---

In addition, a total number of six copulas, including Gaussian, Student t, Clayton, Gumbel, Frank and

Joe copulas, are considered as the candidate models for quantifying the dependence structures for flood

peak-volume at Xianyang and Zhangjiashan gauging stations. Also, the goodness-of-fit statistics is

365   performed based on the Cramér von Mises statistic proposed by Genest et al. (2009). And the indices of

RMSE and AIC would be further employed to evaluate the performance of the obtained copulas and

identify the most appropriate ones. Table 3 shows statistical test results for the selected copulas. The

results show that, for the Zhangjiashan station, all candidate copulas except the Joe copula performed

well, while all six copulas would be able to provide satisfactory risk inferences at the Xianyang station.

370   Moreover, based on the values of RMSE and AIC, the Gumbel copula was chosen to model the

dependence of flood peak and volume at Zhangjiashan station, while the Joe copulas performed best at

the Xianyang station. Consequently, the Gumbel and Joe copula would be chosen in this study to further

characterize the uncertainty in model parameters and the resulting risks at Zhangjiashan and Xianyang

station, respectively.

375

Place Tables 3 here

380

4.2. Uncertainty in Model Parameters and Risk Inferences

Based on the results in Tables 2 and 3, the multivariate risk inference model would be established, in

which the GEV and lognormal distributions would respectively be adopted to model the individual

flood variables at both gauging stations, while in comparison, the Gumbel and Joe copulas would

respectively be employed for Zhangjiashan and Xianyang stations. Afterward, uncertainties would be

characterized based on the bootstrap algorithm illustrated in Section 2.3. In current study, a total number

of 5000 samples would be chosen in order to generally visualize the uncertainty features in model

parameters. The probabilistic features for obtained parameters values (i.e. shape, scale and location for

GEV, meanlog, sdlog for LN, and theta for copula) for each sample scenario would be described by the

kernel method. Figure 3 exhibit the probabilistic distributions for the six unknow parameters in the

established multivariate risk inference model. Extensive uncertainties exist in the parameters for both

the marginal distribution and dependence model. As presented in Figure 3, each parameter, except the

meanlog in the LN distribution, exhibit noticeable uncertainty. Moreover, most of the parameter

uncertainties are approximately normally distributed

Place Figure 3 here

400

It is quite apparent that different parameter values in the copula model would lead to different risk

inference results. Consequently, parameter uncertainties in the marginal distributions and copula

function would definitely result into uncertainties in multivariate risk inferences. Based on the copula

model, some multivariate risk indices can be easily obtained, such as the joint return period in OR,

405   AND and Kendall, as expressed in Equations (12a) – (12c). However, due to parameter uncertainties,

these risk indices may also exhibit some degrees of uncertainty. Figures 4 – 6 describe uncertainties for

the joint RP in AND, OR and Kendall at the two stations. In general, the predictive RP in AND exhibit

most significant uncertainty, followed by the predictive RP in OR and Kendall. However, for moderate

or large flood events, considerable uncertainties can be observed in the inferences for all the three joint

410   RPs. Specifically, noticeable uncertainties exist in the predictive joint RP of AND even for a minor

flood event with a 5-year joint RP. For some large flood events with a joint RP around 100 years, the

predictive RP in AND shows remarkable uncertainty, ranging from less than 50 years to larger than 200

years. For the joint RP in OR and Kendall, slight uncertainty may exist for small flood events (e.g. 2-

year or 5-year joint RP). Nevertheless, apparently uncertainties can be observed in the predictive joint

415   RP even for moderate flood events. As shown in Figure 5, considerable uncertainties may appear in the

predictive joint RP of OR even for a flood with an actual joint RP of 20 years, while prediction of the

Kendall RP for a 20-year (in Kendall RP) flood event may range from 10 to 50 years, as presented in

Figure 6.

420   ---------------------------------

Place Figures 4-6 here

4.3 Individual and Interactive Effects of Parameter Uncertainties

425

It has been observed that parameter uncertainties in the copula-based multivariate risk model would

Hydrology and
Earth System
Sciences
Open Access
EGU
Discussions

lead to significantly imprecise risk predictions. However, one critical issue to be addressed is that how the parameter uncertainties and their interaction would influence the risk inference. Consequently, a multilevel factorial analysis, based on Equations (13) and (14) would be proposed to primarily visualize

430 the individual and interactive effects of parameter uncertainties in the marginal and dependence models on the resulting risk inferences. In this study, a total number of 6 parameters (i.e. three from GEV, two from LN, and one from copula) would to be addresses, and based on probabilistic features of these parameters, three quantile levels (i.e. 0.1, 0.5 and 0.9) would be chosen to characterize the resulting risk inferences under different parameter values. This would finally form a 3^6 factorial design, which has six

435 factors with each having three levels. The failure probability denoted as Equations (11) would be considered as the responses in this factorial design.

The main and interactive effects of parameters uncertainties on the failure probabilities in AND are visualized in Figure 7. It is noticeable that at the two gauge stations, parameters uncertainties pose

440 similar main and interactive effects on the failure probabilities in AND, which indicates that parameters' effects (individual and interactive) on the failure probability in AND are independent with the location of gauge stations. More specifically, variations in the shape parameter in GEV and sdlog parameter in LN would lead to more changes in the corresponding responses (i.e. failure probability in AND) than the variations in other parameters. Also, as shown in Figure 7, the parameter in the copula function (i.e.

445 Cop_theta) describing dependence of the two flood variables, would not have an effect on the resulting risk as visible as the effects from the parameters (except the location parameter in GEV) in the marginal distributions. In terms of parameter interactions, the significance of interactive effects for different parameters is various. The interactive curves for some parameters (e.g. GEV_shape and GEV_location) are nearly parallel at the three levels, indicating an insignificant interaction for these two parameters on

450 the inferred risk. In comparison, there are also some interactive curves intersecting among each other (e.g. GEV_shape and LN_meanlog), implying a significant interaction among these two parameters.

Table 4 provides the results from an ANOVA table for the failure probability in AND. It is quite interesting that: i) even though the effect from the parameter in the copula function is not as visible as the effects from the parameters (except the location parameter in GEV) in the marginal distributions (as shown in Figure 7), such an effect is still statistically significant; i) the effect from the location parameter of GEV is statistically insignificant, which also lead to insignificant interactive effects between the location parameter and other parameters; iii) the interactions between the parameter in copula and the parameters in marginal distributions would be more likely statistically insignificant; iv) the statistical significance (significant or not) for individual and interactive effects from parameters is almost the same between these two gauge stations. All these conclusions obtained from Table 4 are consistent with the implications described in Figure 7.

Place Figures 7 and Table 4 here

In terms of the failure probabilities in OR and Kendall, as presented in Figures 8 and 9, these have similar patter with the failure probability in AND (presented in Figure 7). The individual/main effects from the marginal distributions (except the location parameter in GEV) are generally more visible than the parameter in copula. Also, some interactive curves, especially the curves between GEV_location and others, are parallel, showing insignificant interaction between those parameters. More detailed characterization of the main and interactive effects for the failure probabilities in OR and Kendall is described in the ANOVA tables in Tables 5 and 6. These two tables show some slight differences from the conclusions given by Table 4. The location parameter in GEV also pose statistically significant effect on the results failure probabilities in OR and Kendall, which also leads to some significant interactions between this parameter and other model parameters. For the failure probability in Kendall,

21

the parameter in copula would have more interactions with other parameters in marginal distributions

than the interactions in the failure probability in AND and OR. As presented in Table 6, the parameter in

copula would have statistically significant effect on the inferred failure probability in Kendall with other

480   parameters except the location parameter in GEV. These results are also implied in the main effects

plots and full interactions plot matrices in Figures 8 and 9.

Place Figures 8-9 and Table 5 - 6 here

485   ---

Based on the three-level factorial analysis, it can be generally concluded that the parameters in marginal

distributions (except the location parameter in GEV) would have more individual effects on joint risk

inference than the parameter in copula. The risk indices (i.e. AND, OR, or Kendall) would not have

490   significantly influence the individual effects of model parameters. However, for the interactive effects

among model parameters, they may exhibit slightly different patterns. Specifically, the parameter in

copula would have more significant interactions with parameters in marginal distributions on the failure

risk in Kendall than the other two risk indices. Moreover, the individual and interactive effects from

model parameters on risk inferences would not influence by the location of gauge stations.

495

4.4. Contribution Partition of Uncertainty Sources

As a result of parameter uncertainties, the predictive failure probabilities exhibit noticeable

uncertainties, as shown in Figures 4-6. The three-level factorial analysis based on Equations (11) is able

500   to provide a primary description and visualization related to the individual and interactive effects of

parameter uncertainty on the inferred failure probabilities. However, two critical issues be answered

are: (i) how much would parameter uncertainties contribute to the variation of the inferred risk values? and (ii) do these contributions change significantly for failure probabilities with different service time scenarios? To address these two issues and get reliable results, a full-subsampling factorial approach

505   (FSFA) has been proposed, which would be formulated as Equations (16) – (20). Also, similar with the three-level factorial analysis, three quantile levels would be selected at 0.1, 0.5, and 0.9. Based on FSFA, each parameter at its three quantile values (0.1, 0.5, 0.9) would be further subsampled into three scenarios of two quantile values (i.e. (0.1, 0.5), (0.1, 0.9), and (0.5, 0.9)). For this study, we have a total number of 6 parameters with each choose its three quantile values at 0.1, 0.5, and 0.9, which would lead

510   to a total number of 729 (i.e. 3^6) two-level factorial designs.

In order to be accurate, Figs 10 to 12 are tables and should be labelled and referred to as such....

Figure 10 shows the detailed contributions of the model parameters on uncertainty in predictive failure probabilities of AND at the two gauge stations. It can be observed that, even though some discrepancies exist at Zhangjiashan and Xingshan stations, the detailed contributions for each parameter and their

515   interaction show quite similar features between these two stations. In detail, uncertainty in the shape parameter in GEV has the most significant impact on the failure probability in AND, followed by sdlog in LN, parameter interaction, meanlog in LN, and scale parameter in GEV. Moreover, the uncertainty in the parameter in copula would not lead to significant variation in the resulting failure probability predictions in AND, which would merely make a contribution less than 0.5%. Such conclusions are also

520   generally consistent to the ANOVA results presented in Figure 7 and Table 4. Furthermore, as the increase in service time, the contributions of each parameter and their interactions would not vary significantly. Some individual contributions from parameter uncertainties would slightly increase while other individual contributions may slightly decrease. However, the effect from parameter interactions would generally increase as the increase of service time. In comparison, the enhancement in design

525   standard for hydraulic infrastructure would lead to more chance for deceasing in individual effects and, at the same time, increasing in parameter interactions. For instance, as the flood design standard

23

increases from 200-year to 500-year for a hydraulic facility with 30-year service time near the

Zhangjishan station, the interactive effect of model parameters would increase from 15.14% to 18.09%.

530   --

Place Figure 10 here

In terms of the failure probability in OR, the individual and interactive effects of model parameters on

535   predictive risk uncertainties show similar pattern with the parameters' effects on the failure probability

in AND. As shown in Figure 11, the shape parameter in the GEV distribution and the sdlog in the LN

distribution are the two major sources for uncertainties in failure probabilities in OR. However,

compared with the failure probability in AND, parameter interaction has a less effect on the resulting

uncertainty of risk inference in OR. As shown in Figures 10 and 11, the effect of parameter interaction

540   on the risk in AND ranges between 13.96% and 20.05%, while in comparison, the parameters'

interactive effect on the risk in OR varies within [10.25%, 11.57%]. Apparently, it can also be observed

that some external factors such as the design standard and service time of hydraulic infrastructures have

less influence on the parameters' interaction on risk in OR than the risk in AND. However, the first

contributor (i.e. shape parameter in GEV) would have a more contribution on the predictive uncertainty

545   in the failure probability in OR as the increase in the design standard, while in comparison, this

contributor would have a less contribution on the risk in AND. For instance, as the design return period

of flood (i.e. design standard) increases from 200 to 500 years and the service time of the hydraulic

facility is 30 years, the contribution of the shape parameter in GEV would increase from 47.62% to

50.64% for the failure probability in OR at the Xianyang station, while the parameter's contribution on

550   the failure probability in AND decreases from 49.26% to 45.77%.

Hydrology and
Earth System
Sciences
Discussions

Place Figure 11 here

555

For the failure probability in Kendall, the contributions of model parameters and their interaction are

presented in Figure 12. Similar with the failure probabilities in AND and OR, the shape parameter in the

GEV distribution and the sdlog parameter in the LN distribution are the two major contributors, which

can account for nearly 70% or more in the predictive uncertainty of the failure probability in Kendall.

560   Meanwhile, the scale parameter in GEV, meanlog in LN, and parameters' interaction also have

noticeable effects on the risk in Kendall, ranging from 4.72% (scale parameter in GEV) to 12.64%

(mean log in LN). Conversely, the location parameter in GEV and dependence parameter in copula

merely have quite minor individual effects. However, it is noticeable that, although the dependence

parameter has a minor effect ([0.78%, 1.03%) on the risk in Kendall, such an effect is much higher than

565   the effect on the risk in AND (less than 0.23%) and the risk in OR (less than 0.06%).

Place Figure 12 here

570

Even through the prediction equations for the failure probabilities in AND, OR and Kendall, as

presented in Equations (12) are different, the impacts of parameter uncertainties show quite similar

features, in which the shape parameter in GEV and the sdlog in LN are the two major contributors to the

predictive uncertainties in risk inferences. Nearly 70% and more variability in the uncertainties in risk

inferences can be accounted by the uncertainties in the shape parameter in GEV and sdlog parameter in

575   LN. Also some external factors such as flood design and facility service time may have different

25

influence for parameters' effects on different risk indices, such influence is not significant and would

not lead to remarkable changes in parameters' contribution to risk inferences. Parameters' interaction

has a more effect on risk inference in AND than the other two risk indices (i.e. OR, Kendall), while the

580   contribution from the dependence parameter, even though not noteworthy, has a more effect on the risk

inference in Kendall.

5. Discussion

5.1. Contribution Partition of Uncertainty Sources through Different Approaches

585

In current study, the individual and interactive contributions of parameter uncertainties are quantified

through the developed FSFA approach, in which each parameter has three levels (i.e. 0.1, 0.5, 0.9

quantiles) to be subsampled. In fact, the parameters' contribution can also be characterized by

traditional factorial analysis (FA) approach based on Equations (15) as well as the FSFA approach with

590   more factor levels (e.g. 4 or 5 levels for each parameter).

Figure 13 shows the comparison of parameter contributions to predictive uncertainty for failure

probabilities in AND at Zhangjiashan station for three and four parameter levels scenarios for the design

standard of 200-year. The results of Figure 13(b) are obtained through the FSFA approach with each

595   parameter having four levels to be its quantiles at 0.1, 0.35, 0.6, 0.85. Also, Table 7 presents the

parameter contributions to predictive uncertainty in failure probabilities obtained by traditional FA

approach for Zhangjiashan stations with the design standard of 200-year and service time of 30-year.

Place Figure 13 and Table 7 here

600   --

It can be observed that for different subsampling scenarios, the resulting contributions may be different. However, such a difference would be tolerant since (1) the variations of parameters' contribution are relatively small and mainly happen for the first two contributors, (2) the total contribution of the first

605   two contributors does not change remarkably (around 70% in total), (3) the contributions of other factors especially the parameters' interaction do not vary significantly, and (4) the rank of the contributions from different sources does not change for the two subsampling scenarios. In comparison, as presented in Table 7, the contribution partition of parameter uncertainties obtained through traditional FA shows totally different patterns for different risk inferences. Specifically, traditional FA approach

610   would significantly overestimate parameter interactive effect on risk inference in AND, while at the same time, underestimate the interactive effect on risk inference in OR and Kendall. Consequently, the contribution rank of parameter uncertainties from traditional FA is different from the results obtained through the developed FSFA approach.

615   As shown in Figure 13, the proposed FSFA approach may lead to slightly different results for different subsampling schemes (four or five levels). However, increase in parameter level would highly increase computational demand. For instance, if each parameter has four levels, FSFA approach would lead to a total number of 46,656 (i.e. 6^6) two-level factorial designs. Moreover, the subsampling scheme for factors with five levels would lead to a total number of one million (i.e. 6^{10}) two-level factorial designs.

620   Consequently, the three-level subsampling scheme would generally be recommended and also can generate acceptable results.

5.2. Correlation among Parameters' Contributions

625   The proposed FSFA approach would generally produce a great number of two-level factorial designs. For one specific factor (e.g. GEV_shape), it would have two levels (lower and upper levels) for all

factorial designs. However, the detailed value for the lower or upper level may be different in different

factorial designs. This may finally lead to different contributions for this factor. Figure 14 presents the

variations of parameters' contributions to the prediction of failure probabilities in AND, OR, and

630   Kendall. We already concluded that the shape parameter in GEV (i.e. GEV_shape) and the sdlog in LN

(i.e. LN_sdlog) distribution would generally have the most significant contributions to predictive

uncertainties in risk inferences. However, as shown in Figure 14, the detailed contributions for these

two parameters would vary remarkably for different level values in different factorial designs. In

comparison, the contributions from other parameters and their interaction have less fluctuation than the

635   individual contributions of GEV_shape and LN_sdlog. For instance, although the meanlog in LN (i.e.

LN_meanlog), with a average contribution more than 10%, may have some chances to pose a

predominant contribution more than 50%, most of its contribution are positively distributed within [0,

25%]. Also, even though the parameters' interaction has a noteworthy average contribution larger than

10%, all the detailed contributions in different factorial designs are located within [0, 25%].

640

Place Figure 14 here

----

645   It has been observed that the parameters' contribution may vary significantly due to the differences in

factor values in different factorial designs. One potential issue to be addressed is that how those

individual and interactive contributions correlate each other. Figure 15 presents the Pearson's

correlation among individual and interactive contributions of model parameters to different risk

inferences (i.e. failure probabilities in AND, OR, and Kendall). It is noticeable that the parameters in the

650   LN distribution (i.e. LN_sdlog, LN_meanlog) are generally negatively correlated with the parameters in

the GEV distribution (i.e. GEV_shape, GEV_scale, and GEV_location). Also, for one marginal

Hydrology and
Earth System
Sciences
Discussions

distribution (LN or GEV), its parameters are positively correlated. This implies that an increase in the

contribution of one parameter would lead to a contribution increase for parameters within the same

distribution and at the same time result in a contribution decrease for all parameters in the other

655 distribution. Moreover, if statistically significant, the contribution of the dependent parameter (i.e.

parameter in copula) generally has positive correlation with the contributions from other parameters

except GEV_shape and parameters' interaction. Also, the contribution from parameters' interaction are

generally negatively correlated with the individual contributions from other parameters if such

correlation is statistically significant.

660

Place Figure 15 here

----

665 The proposed FSFA approach can generally characterize how parameter uncertainties would influence

the predictive uncertainties in risk inferences. A large number of two-level factorial designs would be

produced due to different subsampling procedures and then generate different partition results for

parameters' contributions. However, for different risk inferences (i.e. failure probabilities in AND, OR,

and Kendall), these partition results have similar variation features and also show similar correlation

670 plots.

6. Conclusions

Uncertainty quantification is an essential issue for both univariate and multivariate hydrological risk

675 analysis. A number of research works have been posed to reveal uncertain features in multivariate

hydrological risk inference. However, it is required to know the major sources/contributors for

predictive uncertainties in multivariate risk inferences. In this study, a full-subsampling factorial copula

approach (FSFC) has been proposed for uncertainty quantification and partition in multivariate

hydrologic risk inference. In FSFC, a copula-based multivariate risk model has been developed and the

680　　bootstrap method is adopted to quantify the probabilistic features for the parameters in both marginal

distributions and the dependence model. A full-subsampling factorial analysis (FSFA) approach is

finally developed to diminish the effect of the sample size in traditional ANOVA and provided reliable

contribution partition for parameter uncertainties in different risk inferences.

685　　This study is the first attempt to characterize parameter uncertainties in a copula-based multivariate

hydrological risk model and further reveal their contributions to predictive uncertainties for different

risk inferences. As an improvement of ANOVA, the developed FSFA method can mitigate the effect of

bias variance estimation in ANOVA and generate reliable results. Moreover, another noteworthy feature

for the FSFA approach is that it cannot only characterize the impacts for continuous factors (e.g. model

690　　parameters in this study), but also reveal the impacts of discrete or non-numeric factors. Such a feature

can allow the proposed FSFA approach to be employed to further explore the impacts of non-numeric

factors (e.g. model structures, sample size) in hydrologic systems analysis.

Code and data availability: The flooding data for the studied catchments as well as the associated

695　　code for this study can be gathered upon email request to the corresponding authors

Author contributions. YRF, KH, GHH and YPL designed the research. YRF and FW carried out the

research, developed the model code and performed the simulations. YRF prepared the manuscript with

contributions from all co-authors.

700

Competing interests. The authors declare that they have no conflict of interest.

Hydrology and
Earth System
Sciences
Discussions

References

Bobee, B., Cavidas, G., Ashkar, F., Bernier, J., Rasmussen, P.: Towards a systematic approach to comparing
distributions used in flood frequency analysis, J. Hydrol., 142, 121–136, 1993.

710 Bosshard, T., Carambia M., Georgen K., Kotlarski S., Krahe P., Zappa M., Schar C.,: Quantifying uncertainty sources
in an ensemble of hydrological climate-impact projections. Water Resour. Res., 49(3): 1523-1536,
DOI:10.1029/2011wr011533, 2013.

Chebana F., and Ouarda T.B.M.,: Multivariate quantiles in hydrological frequency analysis. Environmetrics, 22(1), 63-
78, 2011.

715 Cunnane, C.: Statistical distributions for flood frequency analysis. Operational Hydrological Report, No. 5/33, World
Meteorological Organization (WMO), Geneva, Switzerland, 1989.

De Michele C, Salvadori G.: A Generalized Pareto intensity-duration model of storm rainfall exploiting 2-copulas. J.
Geophys. Res., 108(D2), 4067, doi:10.1029/2002JD002534, 2003.

Dung N.V., Merz B., Bardossy A., Apel H.:. Handling uncertainty in bivariate quantile estimation – An application to
720 flood hazard analysis in the Mekong Delta. J. Hydrol., 527, 704-717, 2015.

Du T, Xiong L, Xu CY, Gippel CJ, Guo S, Liu P.: Return period and risk analysis of nonstationary low-flow series
under climate change. J. Hydrol., 527, 234-250, 2015.

Fan Y.R., Huang W.W., Huang G.H., Huang K., Zhou X.,: A PCM-based stochastic hydrologic model for uncertainty
quantification in watershed systems. Stochastic Environ. Res. Risk Assess., 29(3) 915-927, 2015a.

725 Fan Y.R., Huang W.W., Li Y.P., Huang G.H., Huang K.: A coupled ensemble filtering and probabilistic collocation
approach for uncertainty quantification of hydrological models. J. Hydrol., 530, 255-272, 2015b.

Fan Y.R., Huang W.W., Huang G.H., Huang K., Li Y.P., Kong X.M.: Bivariate hydrologic risk analysis based on a
coupled entropy-copula method for the Xiangxi River in the Three Gorges Reservoir area, China, Theor. Appl.
Climatol., 125 (1-2), 381-397, doi:10.1007/s00704-015-1505-z, 2016a

730   Fan Y.R., Huang W.W., Huang G.H., Li Y.P., Huang K.: Hydrologic Risk Analysis in the Yangtze River basin through

           Coupling Gaussian Mixtures into Copulas. Adv. Water Resour., 88, 170-185, 2016b.

        Fan Y.R., Huang G.H., Baetz B.W., Li Y.P., Huang K.,: Development of a Copula‐based Particle Filter (CopPF)

           Approach for Hydrologic Data Assimilation under Consideration of Parameter Interdependence. Water Resour. Res.,

           53(6), 4850-4875, 2017.

735   Fan Y.R., Huang G.H., Zhang Y., Li Y.P.,: Uncertainty quantification for multivariate eco-hydrological risk in the

           Xiangxi River within the Three Gorges Reservoir Area in China, Engineering 4 (5), 617-626, 2018.

        Genest C, Rémillard B, Beaudoin D.: Goodness-of-fit tests for copulas: A review and a power study. Insurance:

           Mathematics and Economics, 44:199-213, 2009.

        Graler B., van den Berg M.J., Vandenberghe S., Petroselli A., Grimaldi S., De Baets B., Verhoest N.E.C.,: Multivariate

740   return periods in hydrology: a critical and practical review focusing on synthetic design hydrograph estimation.

           Hydrol. Earth Syst. Sci. 17: 1281–1296, 2013.

        Huang K., Dai L.M., Yao M., Fan Y.R., Kong X.M.: Modelling dependence between traffic noise and traffic flow

           through an entropy-copula method, J. Environ. Inform., 29(2) 134-151, doi:10.3808/jei.201500302, 2017.

        Kao S.C., Govindaraju R.S.: A copula-based joint deficit index for droughts. J. Hydrol., 380, 121-134, 2010.

745   Karmakar S., Simonovic S.P.: Bivariate flood frequency analysis. Part 2: a copula-based approach with mixed marginal

           distributions. J. Flood Risk Manage., 2, 32-44, 2009.

        Kidson R., Richards K.S.: Flood frequency analysis: assumption and alternatives. Prog. Phys. Geogr., 29(3), 392-410,

           2005.

        Kong X.M., Zeng X.T., Chen C., Fan Y.R., Huang G.H., Li Y.P., Wang C.X.: Development of a Maximum Entropy-

750   Archimedean Copula-Based Bayesian Network Method for Streamflow Frequency Analysis—A Case Study of the

           Kaidu River Basin, China, Water, 11(1), 42, 2019

        Kong X.M., Huang G.H., Fan Y.R., Li Y.P.: Maximum entropy-Gumbel-Hougaard copula method for simulation of

           monthly streamflow in Xiangxi river, China. Stochastic Environ. Res. Risk Assess., 29, 833-846, 2015

        Lee T, Salas JD.: Copula-based stochastic simulation of hydrological data applied to Nile River flows. Hydrol. Res.

755   42(4): 318–330, 2011.

        Ma M., Song S., Ren L., Jiang S., Song J.: Multivariate drought characteristics using trivariate Gaussian and Student

           copula. Hydrol. Processes, 27, 1175-1190, 2013.

Merz B, Thieken A.H.: Separating natural and epistemic uncertainty in flood frequency analysis. J. Hydrol., 309(1–4):114–132, 2005.

760   Montgomery, D. C. (Eds.). Design and analysis of experiments (5th ed.). New York: John Wiley & Sons Inc., 2001.

Nelsen R.B., (Eds.). An Introduction to Copulas. Springer: New York, 2006.

Qi, W., Zhang, C., Fu, G., Zhou, H.: Imprecise probabilistic estimation of design floods with epistemic uncertainties. Water Resour. Res., 52(6), 4823–4844, doi:10.1002/2015WR017663, 2016a.

Qi, W., Zhang, C., Fu, G., Zhou, H.: Quantifying dynamic sensitivity of optimization algorithm parameters to improve
765   hydrological model calibration. J. Hydrol., 533: 213-223, DOI:10.1016/j.jhydrol.2015.11.052, 2016b

Requena A., Mediero L., Garrote L.: A bivariate return period based on copulas for hydrologic dam design: Accounting for reservoir routing in risk estimation. Hydrol. Earth Syst. Sci. 17(8):3023-3038, 2013.

Reddy M.J., Ganguli P.: Bivariate flood frequency analysis of Upper Godavari River flows using Archimedean copulas. Water Resour. Manage. 26 (14), 3995-4018, 2012

770   Sadegh M., Ragno E., AghaKouchak, A.: Multivariate Copula Analysis Toolbox (MvCAT): Describing dependence and underlying uncertainty using a Bayesian framework, Water Resour. Res., 53, 5166–5183, doi:10.1002/2016WR020242, 2017

Salvadori G., De Michele C., Durante F.: On the return period and design in a multivariate framework. Hydrol. Earth Syst. Sci. 15: 3293–3305, 2011

775   Salvadori, G., F. Durante, C. De Michele, M. Bernardi, and L. Petrella: A multivariate copula-based framework for dealing with hazard scenarios and failure probabilities, Water Resour. Res., 52, 3701–3721, doi:10.1002/2015WR017225, 2016

Salvadori G., De Michele C., Kottegoda N.T., Rosso R., (Eds.). Extremes in Nature: an Approach using Copula. Springer: Dordrencht; 2007.

780   Sarhadi, A., D. H. Burn, M. C. Ausín, and M. P. Wiper: Time-varying nonstationary multivariate risk analysis using a dynamic Bayesian copula, Water Resour. Res., 52, 2327–2349, doi:10.1002/2015WR01852, 2016

Song J, Xu Z, Liu C, Li H.: Ecological and environmental instream flow requirements for the Wei River – the largest tributary of the Yellow River. Hydrol. Processes, 21, 1066-1073, 2007

Song S., Singh V.P.: Meta-elliptical copulas for drought frequency analysis of periodic hydrologic data. Stochastic

785   Environ. Res. Risk Assess., 24(3), 425-444, 2010.

Sraj M., Bezak N., Brilly M.: Bivariate flood frequency analysis using the copula function: a case study of the Litija

station on the Sava River. Hydrol. Processes, 29(2), 225-238, 2014.

The European Parliament and The Council: Directive 2007/60/EC: On the assessment and management of flood risks,

Official Journal of the European Union, 116 pp, 2007

790   Vandenberghe S, Verhoest NEC, De Baets B.: Fitting bivariate copulas to the dependence structure between storm

characteristics: a detailed analysis based on 105 year 10 min rainfall. Water Resour. Res., 46. DOI:

10.1029/2009wr007857, 2010.

Xu Y., Huang G.H., Fan Y.R.: Multivariate flood risk analysis for Wei River. Stochastic Environ. Res. Risk Assess., 31

(1), 225-242 doi: 10.1007/s00477-015-1196-0, 2016

795   Yue S.: The bivariate lognormal distribution to model a multivariate flood episode. Hydrol. Processes, 14(14), 2575-

2588, 2000

Yue S.: A bivariate gamma distribution for use in multivariate flood frequency analysis. Hydrol. Processes, 15(6),

1033-1045, 2001

Zhang L, Singh VP: Bivariate rainfall frequency distributions using Archimedean copulas. J. Hydrol., 332(1–2):93–

800   109, 2007.

Zhang Q., Xiao M.Z., Singh V.P.: Uncertainty evaluation of copula analysis of hydrological droughts in the East River

basin, China. Global Planet. Change, 129, 1-9, 2015.

Captions of Tables

Table 1. Flood characteristics for different stations

Table 2. Statistical test results for marginal distribution estimation: LN means lognormal distribution, P III means Pearson Type III distribution, and LP III means log-Pearson Type III distribution. K-S test denotes the Kolmogorov–Smirnov test.

Table 3. Performance for quantifying the joint distributions between flood peak and volume through different copulas: CvM is the Cramér von Mises statistic proposed by Genest et al. (2009), with p-value larger than 0.05 indicating satisfactory performance.Table 4. Statistical test results for marginal distribution estimation

Table 4. ANOVA table for failure probability in AND: A indicates the shape parameter in GEV, B indicates the scale parameter of GEV, C indicates the location parameter of GEV, D means the meanlog of LN, E means the sdlog of LN, and F mean the parameters (i.e. theta) in copula Comparison of RMSE and AIC values for joint distributions through different copulas

Table 5. ANOVA table for failure probability in OR: A indicates the shape parameter in GEV, B indicates the scale parameter of GEV, C indicates the location parameter of GEV, D means the meanlog of LN, E means the sdlog of LN, and F mean the parameters (i.e. theta) in copula

Table 6. ANOVA table for failure probability in Kendall: A indicates the shape parameter in GEV, B indicates the scale parameter of GEV, C indicates the location parameter of GEV, D means the meanlog of LN, E means the sdlog of LN, and F mean the parameters (i.e. theta) in

Table 7. Contributions of parameter uncertainties obtained by three level ANOVA to predictive failure probabilities for a design return period of 200-year and service time of 30-year

Captions of Figures

Figure 1: Framework of the proposed FSFC approach

Figure 2. The location of the studied watersheds. Wei River is the largest tributary of Yellow river, with a drainage area of 135,000 km2. The historical flood data from Xianyang and Zhangjiashan stations on the Wei River are analyzed through the proposed FSFC approach. **Figure 3.** Probabilistic features for parameters in marginal distributions and copula: for both Xianyang and Zhangjiashan stations, the GEV (parameters include shape, scale and location) function would be employed to quantify the distribution of flood peak, while the lognormal distribution (parameters denoted as meanlog and sdlog) is applied for flood volume. The Gumbel and Joe copula (parameter denoted as theta) would be respectively adopted to model the dependence between flood peak and volume at Zhangjiashan and Xianyang stations.

Figure 4. Uncertainty quantification of the joint RP in "AND": the red dash lines indicate the predictive means, the two blue dash lines respectively indicate the 5% and 95% quantiles, and the grey lines indicate the predictions under different parameter samples with the same joint RP of the red and blue

840   dash lines; The cyan lines denote the predictions under different return periods with the model
parameters being their mean values.

Figure 5. Uncertainty quantification of the joint RP in "OR": the red dash lines indicate the predictive
means, the two blue dash lines respectively indicate the 5% and 95% quantiles, and the grey lines
indicate the predictions under different parameter samples with the same joint RP of the red and blue

845   dash lines; The cyan lines denote the predictions under different return periods with the model
parameters being their mean values.

Figure 6. Uncertainty quantification of the joint RP in "Kendall": the red dash lines indicate the predictive
means, the two blue dash lines respectively indicate the 5% and 95% quantiles, and the grey lines indicate
the predictions under different parameter samples with the same joint RP of the red and blue dash lines;

850   The cyan lines denote the predictions under different return periods with the model parameters being their
mean values

Figure 7. Main effects plot and full interactions plot matrix for parameters on the failure probability in
AND at the two gauge stations

Figure 8. Main effects plot and full interactions plot matrix for parameters on the failure probability in
855   OR at the two gauge stations

Figure 9. Main effects plot and full interactions plot matrix for parameters on the failure probability in
Kendall at the two gauge stations

Figure 10. Contributions of parameter uncertainties to predictive failure probabilities in AND under
different design standards (i.e. return periods (RP)) and different service periods

860   **Figure 11.** Contributions of parameter uncertainties to predictive failure probabilities in OR under
different design standards (i.e. return periods (RP)) and different service periods

Figure 12. Contributions of parameter uncertainties to predictive failure probabilities in Kendall under
different design standards (i.e. return periods (RP)) and different service periods

Figure 13. Comparison of parameter contributions to predictive uncertainty for failure probabilities
865   under different levels of subsampling for Zhangjiashan station: three (i.e. 0.1, 0.5, 0.9) and four (i.e. 0.1,
0.35, 0.6, 0.85) level quantiles are adopted for subsampling and the design return period is 200 years.

Figure 14. Variation of parameters' contributions for different risk inferences at the Zhangjiashan
Station for a design standard of 200-year and a service time of 30-year

Figure 15. Correlation for parameters' contributions on risk inferences at Zhangjiashan station for a
870   design standard of 200-year and a service time of 30-year: The cross sign indicates the correlation is
statistically insignificant

Table 1. Flood characteristics for different stations

Station name	period		flood variable	
			Peak (m^3/s)	Volume (m^3/(s day))
		Minimum	139	317
Xianyang	1960-2006	Median	1350	2491
		Maximum	12380	17802
		Minimum	217	303.7
Zhangjiashan	1958-2012	Median	775	1365.3
		Maximum	3730	7576.1

875

Table 2. Statistical test results for marginal distribution estimation: LN means lognormal distribution, P III means Pearson Type III distribution, and LP III means log-Pearson Type III distribution. K-S test denotes the Kolmogorov–Smirnov test.

Station name	Flooding variables	Marginal distribution	K-S test		RMSE	AIC
			T	P-value		
Zhangjiashan	Peak	Gamma	0.0745	0.5471	0.0378	-323.5512
		GEV	**0.0724**	**0.9151**	**0.0275**	**-389.3956**
		LN	0.0805	0.8403	0.0283	-388.3297
		P III	0.0893	0.7386	0.0395	-349.3274
		LP III	0.0795	0.8508	0.0324	-371.3614
	Volume	Gamma	0.1460	0.1735	0.0596	-306.2925
		GEV	0.1017	0.5839	0.0369	-357.0852
		LN	**0.0904**	**0.7250**	**0.0361**	**-361.3353**
		P III	0.1589	0.1112	0.0737	-280.8701
		LP III	0.0967	0.6468	0.0367	-357.5476
Xianyang	Peak	Gamma	0.1159	0.5533	0.0372	-305.4087
		GEV	**0.0875**	**0.8645**	**0.0305**	**-321.9202**
		LN	0.1051	0.6763	0.0436	-290.5248
		P III	0.1202	0.5051	0.0416	-292.8448
		LP III	0.1321	0.3848	0.0617	-255.8931
	Volume	Gamma	0.1146	0.5305	0.0450	-287.4880
		GEV	0.0540	0.9980	0.0195	-364.3058
		LN	**0.0670**	**0.9749**	**0.0192**	**-367.3885**
		P III	0.1005	0.6913	0.0377	-302.0492
		LP III	0.0722	0.9522	0.0313	-319.6540

Table 3. Performance for quantifying the joint distributions between flood peak and volume through different copulas: CvM is the Cramér von Mises statistic proposed by Genest et al. (2009), with p-value larger than 0.05 indicating satisfactory performance.

		RMSE	AIC	CvM	p-value
Zhangjiashan	Gaussian	0.0669	-295.5144	7.9302	0.7770
	Student t	0.0669	-293.5237	8.5203	0.5976
	Clayton	0.0843	-270.0616	9.4615	0.3290
	Gumbel	**0.0637**	**-300.8577**	**7.9342**	**0.7580**
	Frank	0.0690	-292.0723	9.0704	0.4480
	Joe	0.0606	-306.3185	11.0321	0.0290
Xinshan	Gaussian	0.0513	-277.1704	8.4731	0.2400
	Student t	0.0510	-275.6834	8.2295	0.2885
	Clayton	0.0618	-259.7391	8.2051	0.3240
	Gumbel	0.0477	-283.9933	7.1344	0.6700
	Frank	0.0562	-268.6861	8.2725	0.2940
	Joe	**0.0446**	**-290.2631**	**6.9905**	**0.6540**

Hydrology and
Earth System
Sciences
Discussions

what do the red highlights mean?
what are SS, DF and MS?

Table 4. ANOVA table for failure probability in AND: A indicates the shape parameter in GEV, B indicates the scale parameter of GEV, C indicates the location parameter of GEV, D means the meanlog of LN, E means the sdlog of LN, and F mean the parameters (i.e. theta) in copula

Parameter	Zhangjiashan					Xianyang				
	SS	DF	MS	F-Value	P-value	SS	DF	MS	F-Value	P-value
A	0.37	2	0.18	7512.32	< 0.0001	0.59	2	0.30	5079.77	< 0.0001
B	0.018	2	8.905E-003	362.65	< 0.0001	0.013	2	6.527E-003	111.71	< 0.0001
C	8.313E-005	2	4.156E-005	1.69	0.1849	8.642E-005	2	4.321E-005	0.74	0.4777
D	0.059	2	0.029	1195.61	< 0.0001	0.082	2	0.041	701.54	< 0.0001
E	0.18	2	0.092	3766.70	< 0.0001	0.31	2	0.16	2656.85	< 0.0001
F	9.379E-004	2	4.690E-004	19.10	< 0.0001	7.813E-004	2	3.907E-004	6.69	0.0013
AB	2.874E-003	4	7.186E-004	29.26	< 0.0001	8.730E-003	4	2.183E-003	37.35	< 0.0001
AC	1.179E-005	4	2.948E-006	0.12	0.9753	5.434E-005	4	1.359E-005	0.23	0.9201
AD	0.047	4	0.012	473.52	< 0.0001	0.079	4	0.020	338.27	< 0.0001
AE	0.14	4	0.036	1448.10	< 0.0001	0.28	4	0.070	1193.40	< 0.0001
AF	4.311E-004	4	1.078E-004	4.39	0.0017	4.687E-004	4	1.172E-004	2.01	0.0921
BC	2.905E-007	4	7.263E-008	2.958E-003	1.0000	2.235E-008	4	5.588E-009	9.564E-005	1.0000
BD	2.422E-003	4	6.055E-004	24.66	< 0.0001	2.465E-003	4	6.162E-004	10.55	< 0.0001
BE	6.956E-003	4	1.739E-003	70.81	< 0.0001	8.669E-003	4	2.167E-003	37.09	< 0.0001
BF	8.325E-006	4	2.081E-006	0.085	0.9871	2.355E-006	4	5.888E-007	0.010	0.9998
CD	1.143E-005	4	2.859E-006	0.12	0.9767	1.652E-005	4	4.131E-006	0.071	0.9909
CE	3.235E-005	4	8.088E-006	0.33	0.8583	5.669E-005	4	1.417E-005	0.24	0.9142
CF	3.820E-008	4	9.551E-009	3.889E-004	1.0000	1.559E-008	4	3.897E-009	6.670E-005	1.0000
DE	1.792E-003	4	4.481E-004	18.25	< 0.0001	6.919E-003	4	1.730E-003	29.60	< 0.0001
DF	9.625E-005	4	2.406E-005	0.98	0.4178	1.288E-004	4	3.221E-005	0.55	0.6982
EF	3.238E-004	4	8.095E-005	3.30	0.0109	4.540E-004	4	1.135E-004	1.94	0.1017
Error	0.016	656	2.456E-005			0.038	656	5.843E-005		
Total SS	0.85	728				1.42	728			

Table 5. ANOVA table for failure probability in OR: A indicates the shape parameter in GEV, B indicates the scale parameter of GEV, C indicates the location parameter of GEV, D means the meanlog of LN, E means the sdlog of LN, and F mean the parameters (i.e. theta) in copula

Parameter	Zhangjiashan					Xianyang				
	SS	DF	MS	F-Value	P-value	SS	DF	MS	F-Value	P-value
A	2.04	2	1.02	39285.40	< 0.0001	3.71	2	1.85	30534.64	< 0.0001
B	0.20	2	0.098	3784.17	< 0.0001	0.26	2	0.13	2165.79	< 0.0001
C	9.466E-004	2	4.733E-004	18.22	< 0.0001	1.811E-003	2	9.054E-004	14.91	< 0.0001
D	0.24	2	0.12	4679.22	< 0.0001	0.30	2	0.15	2498.09	< 0.0001
E	0.60	2	0.30	11626.79	< 0.0001	0.87	2	0.43	7132.20	< 0.0001
F	7.833E-004	2	3.916E-004	15.08	< 0.0001	6.382E-004	2	3.191E-004	5.26	0.0054
AB	0.17	4	0.043	1666.34	< 0.0001	0.27	4	0.069	1128.63	< 0.0001
AC	8.076E-004	4	2.019E-004	7.77	< 0.0001	1.830E-003	4	4.575E-004	7.54	< 0.0001
AD	0.048	4	0.012	465.73	< 0.0001	0.081	4	0.020	335.01	< 0.0001
AE	0.15	4	0.037	1418.17	< 0.0001	0.29	4	0.071	1175.81	< 0.0001
AF	3.442E-004	4	8.604E-005	3.31	0.0106	3.658E-004	4	9.144E-005	1.51	0.1986
BC	8.013E-005	4	2.003E-005	0.77	0.5442	1.226E-004	4	3.064E-005	0.50	0.7323
BD	2.528E-003	4	6.319E-004	24.33	< 0.0001	2.534E-003	4	6.334E-004	10.43	< 0.0001
BE	7.212E-003	4	1.803E-003	69.40	< 0.0001	8.837E-003	4	2.209E-003	36.39	< 0.0001
BF	5.294E-006	4	1.323E-006	0.051	0.9951	1.077E-006	4	2.693E-007	4.436E-003	1.0000
CD	1.192E-005	4	2.981E-006	0.11	0.9773	1.697E-005	4	4.242E-006	0.070	0.9911
CE	3.353E-005	4	8.382E-006	0.32	0.8628	5.780E-005	4	1.445E-005	0.24	0.9169
CF	2.416E-008	4	6.040E-009	2.325E-004	1.0000	7.119E-009	4	1.780E-009	2.932E-005	1.0000
DE	0.11	4	0.028	1069.79	< 0.0001	0.17	4	0.042	691.60	< 0.0001
DF	7.482E-005	4	1.870E-005	0.72	0.5784	9.919E-005	4	2.480E-005	0.41	0.8026
EF	2.568E-004	4	6.420E-005	2.47	0.0435	3.550E-004	4	8.876E-005	1.46	0.2121
Error	0.017	656	2.598E-005			0.040	656	6.071E-005		
Total SS	3.60	728				6.01	728			

Table 6. ANOVA table for failure probability in Kendall: A indicates the shape parameter in GEV, B indicates the scale parameter of GEV, C indicates the location parameter of GEV, D means the meanlog of LN, E means the sdlog of LN, and F mean the parameters (i.e. theta) in copula

Parameter	Zhangjiashan					Xianyang				
	SS	DF	MS	F-Value	P-value	SS	DF	MS	F-Value	P-value
A	0.97	2	0.48	33813.15	< 0.0001	2.08	2	1.04	27047.85	< 0.0001
B	0.096	2	0.048	3349.45	< 0.0001	0.15	2	0.076	1983.83	< 0.0001
C	4.627E-004	2	2.313E-004	16.19	< 0.0001	1.055E-003	2	5.274E-004	13.72	< 0.0001
D	0.11	2	0.057	3987.58	< 0.0001	0.17	2	0.084	2181.53	< 0.0001
E	0.28	2	0.14	9809.61	< 0.0001	0.47	2	0.24	6153.63	< 0.0001
F	0.013	2	6.451E-003	451.42	< 0.0001	0.025	2	0.013	331.58	< 0.0001
AB	0.087	4	0.022	1525.14	< 0.0001	0.16	4	0.041	1066.18	< 0.0001
AC	4.090E-004	4	1.022E-004	7.15	< 0.0001	1.101E-003	4	2.754E-004	7.16	< 0.0001
AD	0.022	4	5.448E-003	381.22	< 0.0001	0.044	4	0.011	286.00	< 0.0001
AE	0.066	4	0.017	1156.06	< 0.0001	0.15	4	0.038	995.79	< 0.0001
AF	2.163E-003	4	5.407E-004	37.84	< 0.0001	5.986E-003	4	1.496E-003	38.93	< 0.0001
BC	4.233E-005	4	1.058E-005	0.74	0.5645	7.800E-005	4	1.950E-005	0.51	0.7304
BD	1.147E-003	4	2.866E-004	20.06	< 0.0001	1.377E-003	4	3.444E-004	8.96	< 0.0001
BE	3.254E-003	4	8.135E-004	56.93	< 0.0001	4.755E-003	4	1.189E-003	30.93	< 0.0001
BF	2.479E-004	4	6.198E-005	4.34	0.0018	4.939E-004	4	1.235E-004	3.21	0.0126
CD	5.408E-006	4	1.352E-006	0.095	0.9842	9.226E-006	4	2.307E-006	0.060	0.9933
CE	1.513E-005	4	3.782E-006	0.26	0.9007	3.112E-005	4	7.781E-006	0.20	0.9370
CF	1.190E-006	4	2.974E-007	0.021	0.9992	3.369E-006	4	8.423E-007	0.022	0.9991
DE	0.054	4	0.014	950.06	< 0.0001	0.096	4	0.024	623.48	< 0.0001
DF	1.870E-004	4	4.676E-005	3.27	0.0114	3.437E-004	4	8.592E-005	2.24	0.0638
EF	4.113E-004	4	1.028E-004	7.20	< 0.0001	9.130E-004	4	2.282E-004	5.94	0.0001
Error	9.374E-003	656	1.429E-005			0.025	656	3.844E-005		
Total SS	1.72	728				3.40	728			

Table 7. Contributions of parameter uncertainties obtained by three level ANOVA to predictive failure probabilities for a design return period of 200-year and service time of 30-year

Factor	FPand	FPor	FPkendall
A	43.53%	56.67%	56.40%
B	2.12%	5.56%	5.58%
C	0.01%	0.03%	0.03%
D	6.94%	6.67%	6.40%
E	21.18%	16.67%	16.28%
F	0.11%	0.02%	0.76%
Interaction	26.12%	4.72%	5.06%
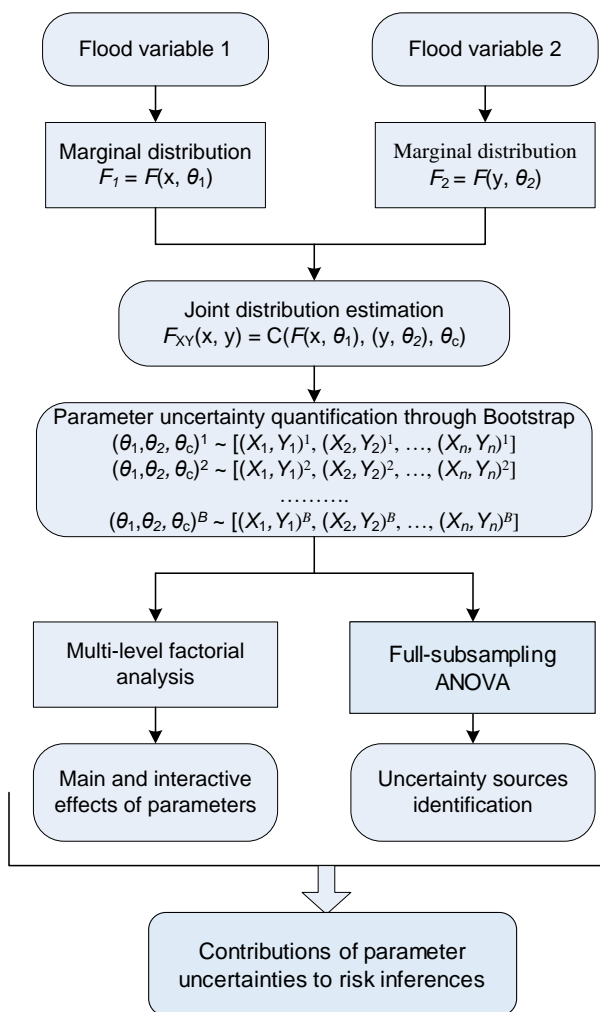
Figure 1. Framework of the proposed FSFC approach.

this is the width of HESS margins

please expand this map about 3 times - on an A4 page the lettering is illegible
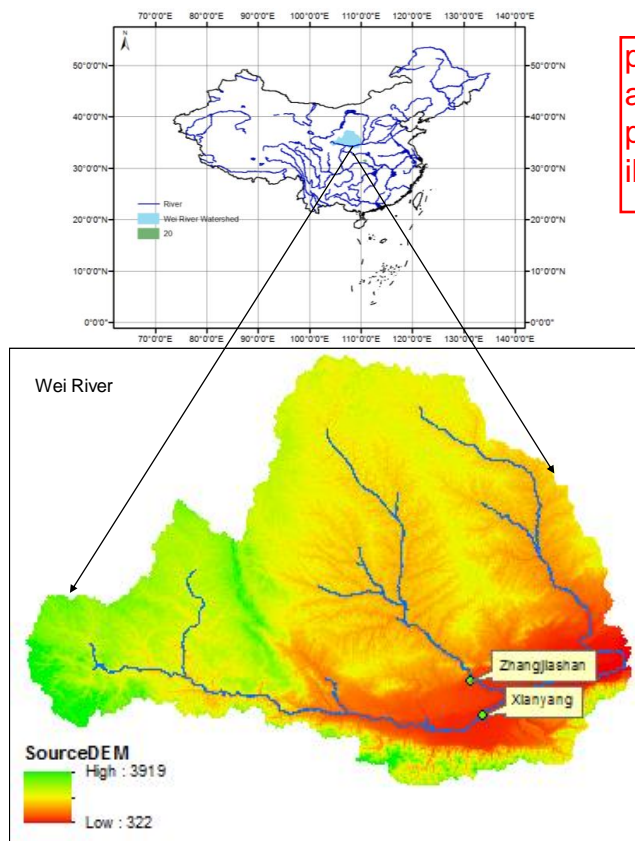
Figure 2. The location of the studied watersheds. Wei River is the largest tributary of Yellow river, with a drainage area of 135,000 km^2. The historical flood data from Xianyang and Zhangjiashan stations on the Wei River are analyzed through the proposed FSFC approach.

Hydrology and
Earth System
Sciences
Discussions

this is the width of HESS margins

please expand this figure - on an A4 page the lettering is very small and hard to read
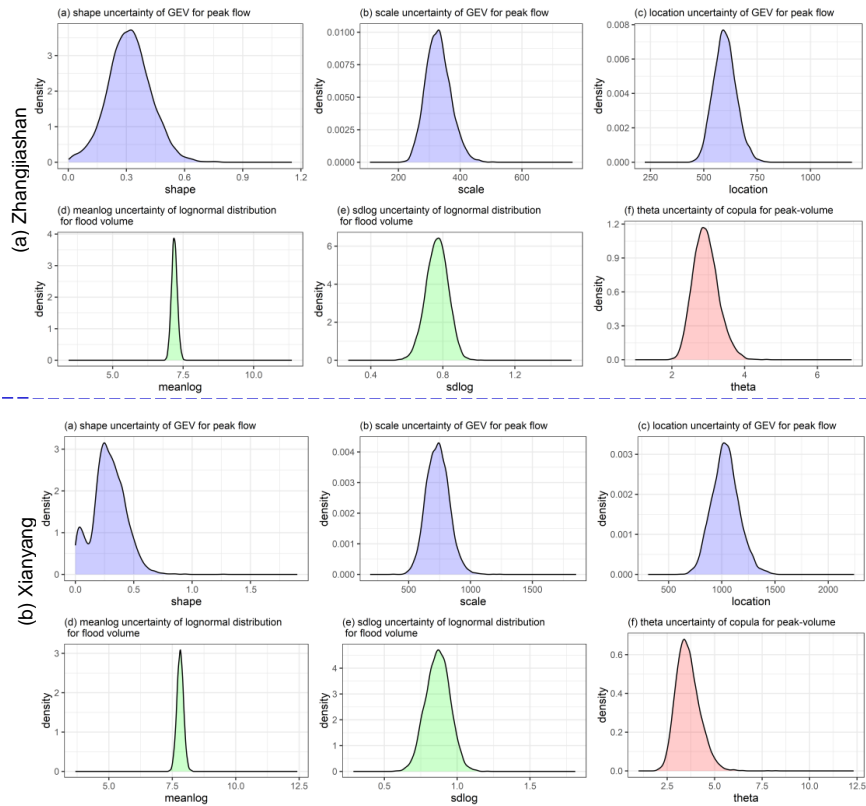
Figure 3. Probabilistic features for parameters in marginal distributions and copula: for both Xianyang and Zhangjiashan stations, the GEV (parameters include shape, scale and location) function would be employed to quantify the distribution of flood peak, while the lognormal distribution (parameters denoted as meanlog and sdlog) is applied for flood volume. The Gumbel and Joe copula (parameter denoted as theta) would be respectively adopted to model the dependence between flood peak and volume at Zhangjiashan and Xianyang stations.

please expand this
figure - on an A4 page
the lettering is very
small
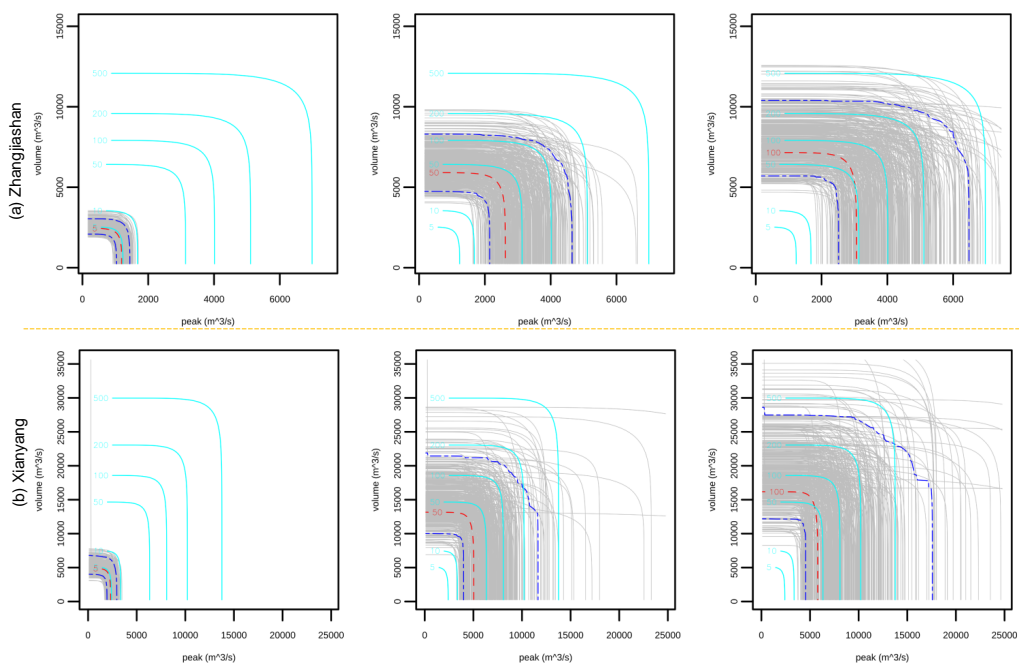
Figure 4. Uncertainty quantification of the joint RP in "AND": the red dash lines indicate the predictive means, the two blue dash lines respectively indicate the 5% and 95% quantiles, and the grey lines indicate the predictions under different parameter samples with the same joint RP of the red and blue dash lines; The cyan lines denote the predictions under different return periods with the model parameters being their mean values.

please expand this figure - on an A4 page the lettering is very small

Figure 5. Uncertainty quantification of the joint RP in "OR": the red dash lines indicate the predictive means, the two blue dash lines respectively indicate the 5% and 95% quantiles, and the grey lines indicate the predictions under different parameter samples with the same joint RP of the red and blue dash lines; The cyan lines denote the predictions under different return periods with the model parameters being their mean values.

please expand this figure - on an A4 page the lettering is very small

Figure 6. Uncertainty quantification of the joint RP in "Kendall": the red dash lines indicate the predictive means, the two blue dash lines respectively indicate the 5% and 95% quantiles, and the grey lines indicate the predictions under different parameter samples with the same joint RP of the red and blue dash lines; The cyan lines denote the predictions under different return periods with the model parameters being their mean values.

please expand this figure - on an A4 page the lettering is very small and the font should be increased in size - it seems this request applies to all figures, but not tables.
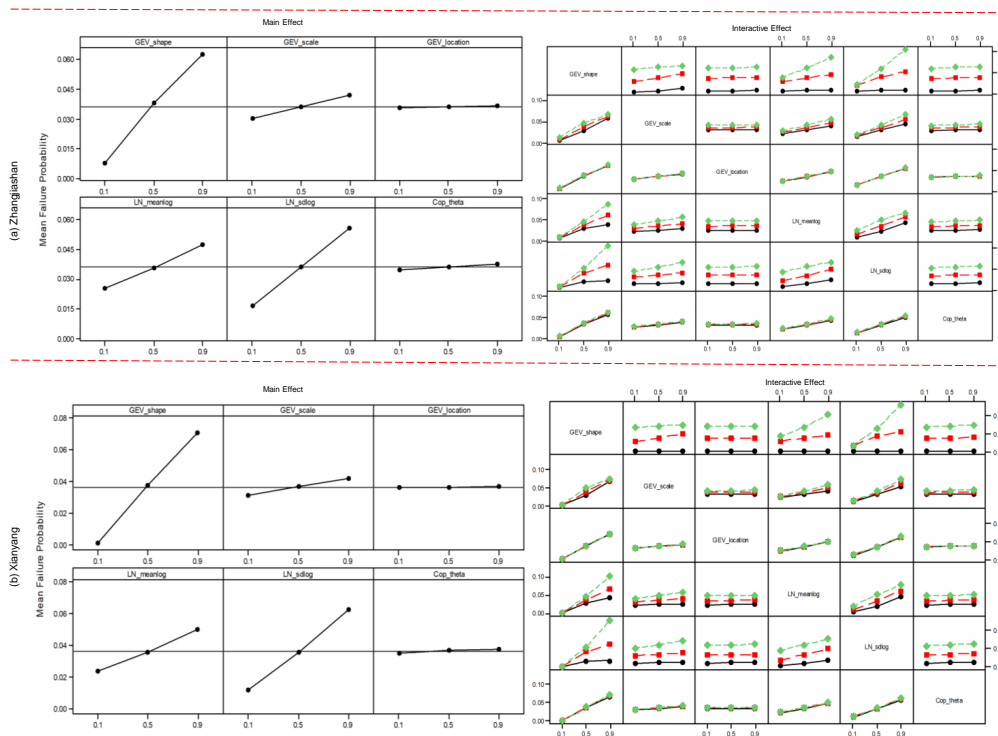
Figure 7. Main effects plot and full interactions plot matrix for parameters on the failure probability in AND at the two gauge stations.

in figures 7 through 9, please add some text in the caption to explain what the figures are showing the reader. In the images of 'interactive effect', why is the labelling put on the diagonal? are the labels describing vertical columns or horizontal rows? what are the green, red and black plots telling us? This layout poses an unnecessary puzzle for the reader.

Figure 8. Main effects plot and full interactions plot matrix for parameters on the failure probability in OR at the two gauge stations

Figure 9. Main effects plot and full interactions plot matrix for parameters on the failure probability in Kendall at the two gauge stations

|		(a) Zhangjiashan			(b) Xianyang		
RP: 200	GEV_shape	45.83%	46.37%	46.88%	49.26%	50.15%	50.99%
	GEV_scale	4.93%	4.96%	5.00%	2.27%	2.24%	2.21%
	GEV_location	0.05%	0.05%	0.05%	0.03%	0.03%	0.03%
	LN_meanlog	10.22%	10.21%	10.19%	8.30%	8.24%	8.19%
	LN_sdlog	23.61%	23.67%	23.70%	23.02%	23.08%	23.11%
	Cop_theta	0.23%	0.23%	0.22%	0.11%	0.10%	0.10%
	Par_interaction	15.14%	14.52%	13.96%	17.02%	16.16%	15.38%
RP: 300	GEV_shape	45.86%	46.30%	46.73%	47.74%	48.40%	49.04%
	GEV_scale	4.04%	4.05%	4.06%	1.95%	1.93%	1.91%
	GEV_location	0.03%	0.03%	0.03%	0.02%	0.02%	0.02%
	LN_meanlog	9.44%	9.43%	9.41%	7.83%	7.78%	7.73%
	LN_sdlog	23.96%	24.03%	24.08%	23.70%	23.79%	23.86%
	Cop_theta	0.18%	0.18%	0.17%	0.09%	0.08%	0.08%
	Par_interaction	16.48%	15.98%	15.51%	18.68%	18.00%	17.36%
RP: 500	GEV_shape	45.50%	45.82%	46.13%	45.77%	46.22%	46.65%
	GEV_scale	3.22%	3.22%	3.21%	1.71%	1.69%	1.67%
	GEV_location	0.02%	0.02%	0.02%	0.01%	0.01%	0.01%
	LN_meanlog	8.66%	8.65%	8.63%	7.36%	7.32%	7.28%
	LN_sdlog	24.38%	24.44%	24.50%	24.43%	24.52%	24.61%
	Cop_theta	0.14%	0.14%	0.13%	0.07%	0.07%	0.06%
	Par_interaction	18.09%	17.72%	17.37%	20.65%	20.18%	19.71%
		30 year	50 year	70 year	30 year	50 year	70 year

Legend: 1%, 10%, 20%, 30%, 40%, 50%

Figure 10. Contributions of parameter uncertainties to predictive failure probabilities in AND under different design standards (i.e. return periods (RP)) and different service periods

		(a) Zhangjiashan			(b) Xianyang		
		30 year	50 year	70 year	30 year	50 year	70 year
RP: 200	GEV_shape	45.60%	45.64%	45.52%	47.62%	47.53%	47.22%
	GEV_scale	6.94%	6.57%	6.23%	5.23%	4.77%	4.37%
	GEV_location	0.07%	0.07%	0.06%	0.07%	0.06%	0.06%
	LN_meanlog	12.60%	12.55%	12.50%	10.96%	10.92%	10.86%
	LN_sdlog	24.48%	24.75%	24.98%	24.51%	24.97%	25.36%
	Cop_theta	0.06%	0.06%	0.06%	0.03%	0.03%	0.03%
	Par_interaction	10.25%	10.37%	10.65%	11.57%	11.73%	12.11%
RP: 300	GEV_shape	46.95%	47.05%	47.05%	49.05%	49.07%	48.96%
	GEV_scale	6.47%	6.16%	5.87%	5.04%	4.64%	4.28%
	GEV_location	0.05%	0.05%	0.04%	0.05%	0.05%	0.04%
	LN_meanlog	11.65%	11.61%	11.58%	10.11%	10.07%	10.04%
	LN_sdlog	24.37%	24.63%	24.86%	24.19%	24.61%	25.00%
	Cop_theta	0.05%	0.04%	0.04%	0.02%	0.02%	0.02%
	Par_interaction	10.47%	10.47%	10.55%	11.54%	11.54%	11.66%
RP: 500	GEV_shape	48.45%	48.56%	48.63%	50.64%	50.73%	50.74%
	GEV_scale	6.01%	5.77%	5.54%	4.85%	4.53%	4.24%
	GEV_location	0.03%	0.03%	0.03%	0.04%	0.03%	0.03%
	LN_meanlog	10.65%	10.62%	10.60%	9.22%	9.20%	9.17%
	LN_sdlog	24.14%	24.35%	24.56%	23.73%	24.07%	24.40%
	Cop_theta	0.03%	0.03%	0.03%	0.02%	0.02%	0.02%
	Par_interaction	10.69%	10.63%	10.61%	11.51%	11.43%	11.41%

Legend: 1% / 10% / 20% / 30% / 40% / 50%

Figure 11. Contributions of parameter uncertainties to predictive failure probabilities in OR under different design standards (i.e. return periods (RP)) and different service periods

		(a) Zhangjiashan			(b) Xianyang		
RP: 200	GEV_shape	45.02%	45.15%	45.21%	47.04%	47.13%	47.09%
	GEV_scale	7.06%	6.82%	6.58%	5.38%	5.04%	4.72%
	GEV_location	0.07%	0.07%	0.07%	0.08%	0.07%	0.06%
	LN_meanlog	12.46%	12.45%	12.43%	10.84%	10.82%	10.79%
	LN_sdlog	24.03%	24.24%	24.43%	24.00%	24.36%	24.70%
	Cop_theta	1.02%	0.98%	0.94%	1.03%	0.96%	0.90%
	Par_interaction	10.33%	10.29%	10.34%	11.64%	11.62%	11.72%
RP: 300	GEV_shape	46.37%	46.51%	46.60%	48.45%	48.57%	48.62%
	GEV_scale	6.57%	6.36%	6.16%	5.16%	4.87%	4.59%
	GEV_location	0.05%	0.05%	0.05%	0.05%	0.05%	0.05%
	LN_meanlog	11.52%	11.51%	11.49%	9.99%	9.98%	9.96%
	LN_sdlog	23.95%	24.14%	24.32%	23.71%	24.04%	24.35%
	Cop_theta	0.94%	0.91%	0.88%	0.94%	0.89%	0.85%
	Par_interaction	10.60%	10.53%	10.51%	11.69%	11.60%	11.58%
RP: 500	GEV_shape	47.89%	48.01%	48.10%	50.03%	50.17%	50.26%
	GEV_scale	6.08%	5.92%	5.77%	4.94%	4.71%	4.49%
	GEV_location	0.03%	0.03%	0.03%	0.04%	0.03%	0.03%
	LN_meanlog	10.54%	10.53%	10.52%	9.13%	9.12%	9.10%
	LN_sdlog	23.76%	23.91%	24.06%	23.30%	23.56%	23.82%
	Cop_theta	0.85%	0.83%	0.80%	0.85%	0.82%	0.78%
	Par_interaction	10.86%	10.78%	10.72%	11.71%	11.59%	11.52%
		30 year	50 year	70 year	30 year	50 year	70 year

Legend: 1%, 10%, 20%, 30%, 40%, 50%

Figure 12. Contributions of parameter uncertainties to predictive failure probabilities in Kendall under different design standards (i.e. return periods (RP)) and different service periods
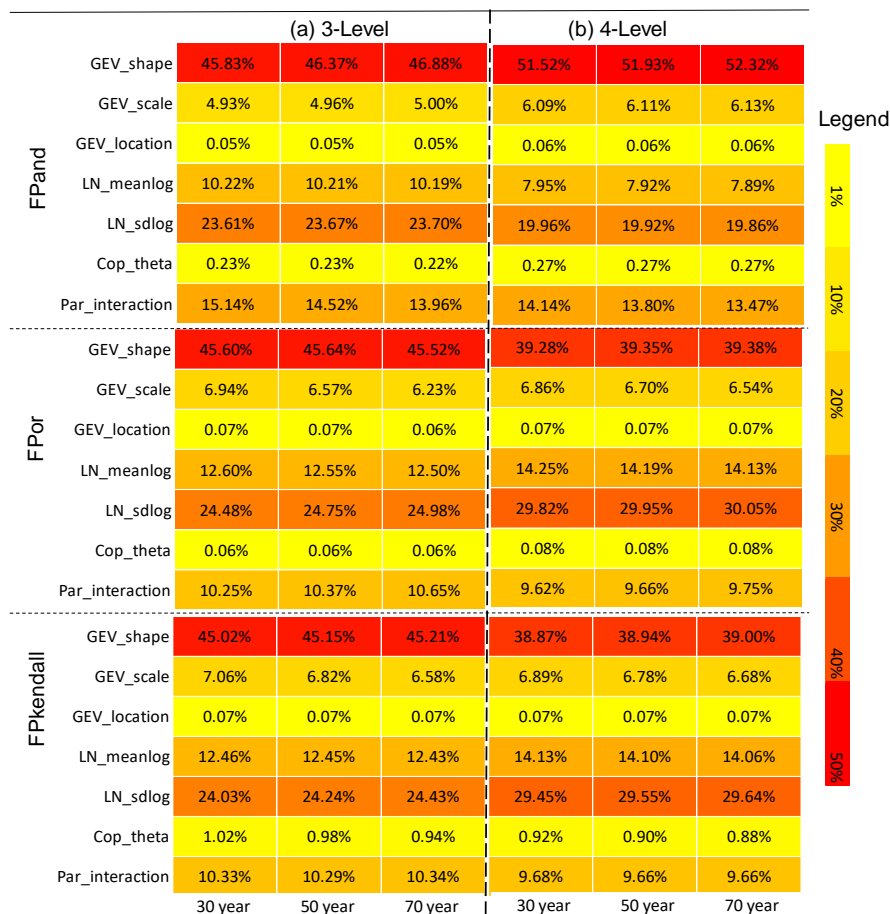
Figure 13. Comparison of parameter contributions to predictive uncertainty for failure probabilities under different levels of subsampling for Zhangjiashan station: three (i.e. 0.1, 0.5, 0.9) and four (i.e. 0.1, 0.35, 0.6, 0.85) level quantiles are adopted for subsampling and the design return period is 200 years.
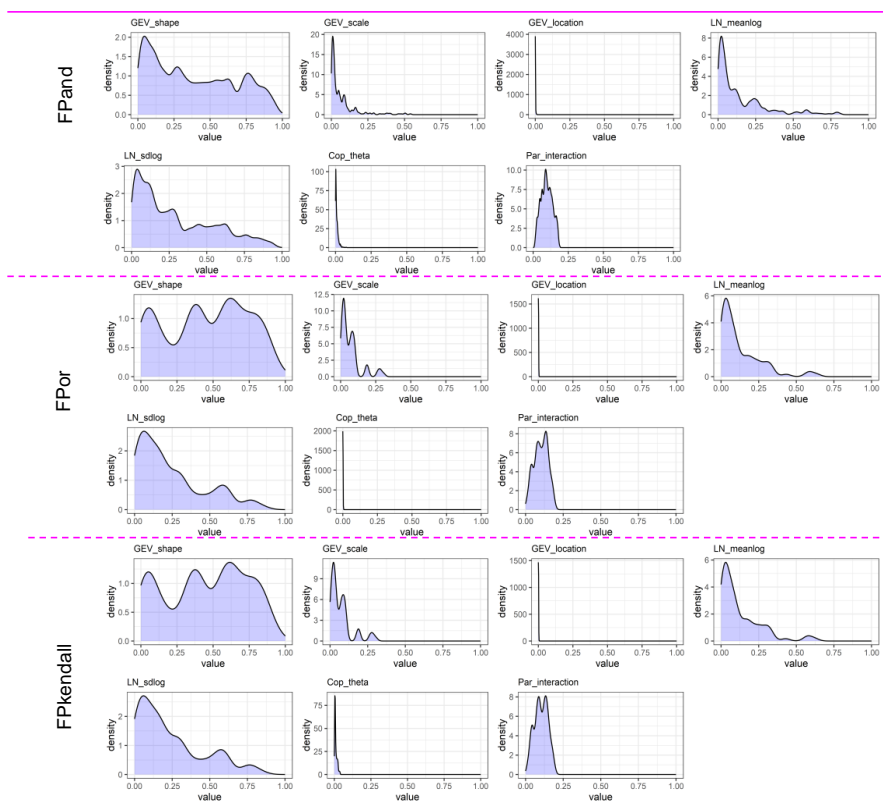
Figure 14. Variation of parameters' contributions for different risk inferences at the Zhangjiashan Station for a design standard of 200-year and a service time of 30-year
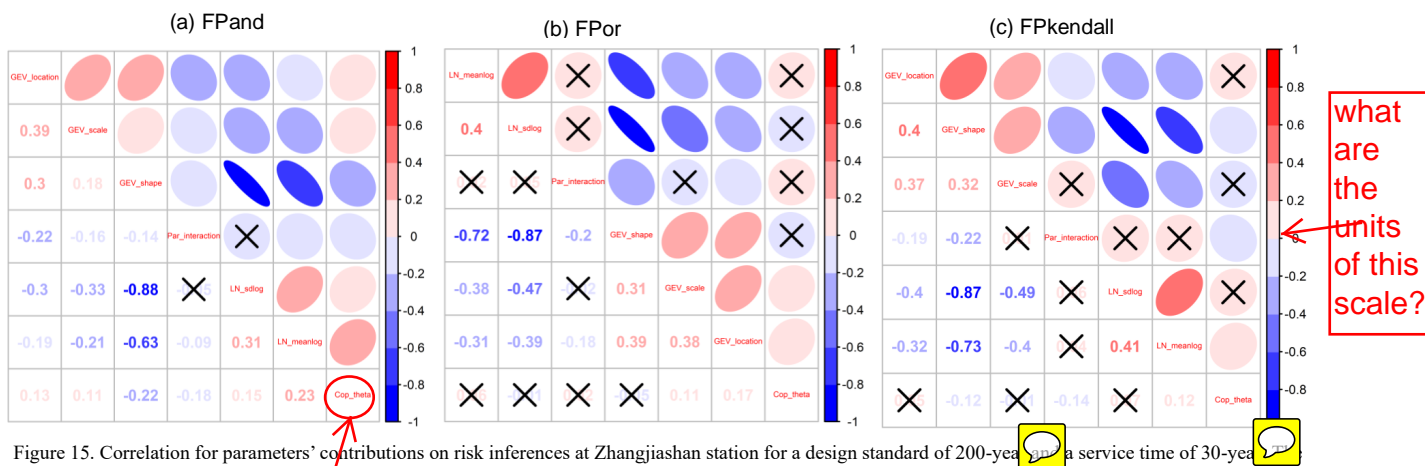
Figure 15. Correlation for parameters' contributions on risk inferences at Zhangjiashan station for a design standard of 200-year and a service time of 30-year. The cross sign indicates the correlation is statistically insignificant.